Outage Probability Analysis of Correlated Sources Transmission over Fading Channels with Line-of-sight Component

Shen Qian

A thesis submitted to
School of Information Science,
Japan Advanced Institute of Science and Technology,
in partial fulfillment of the requirements
for the degree of
Master of Information Science
Graduate Program in Information Science

Written under the direction of
Professor Tadashi Matsumoto

March, 2014

Outage Probability Analysis of Correlated Sources Transmission over Fading Channels with Line-of-sight Component

Shen Qian (1210021)

A thesis submitted to
School of Information Science,
Japan Advanced Institute of Science and Technology,
in partial fulfillment of the requirements
for the degree of
Master of Information Science
Graduate Program in Information Science

Written under the direction of
Professor Tadashi Matsumoto

and approved by
Professor Tadashi Matsumoto
Associate Professor Brian Michael Kurkoski
Professor Mineo Kaneko

February, 2014 (Submitted)

I certify that I have prepared this Master's Thesis by myself without any inadmissible outside help.

Shen Qian
JAIST, Feb, 12, 2014

Author : _____

Date : _____

Supervisor : _____

Acknowledgments

About two years ago, I made the one of the most important decisions in my life. I decided to go back to school for advance studying, after leaving college almost ten years ago. Now, it has been proven that the decision made two years ago is very correct and valuable. This two years of the study life is very important and will make significant and profound impact my future life.

I was very lucky that I joined a very aggressive team with many talented and kind members. They are very friendly and brilliant. Especially My supervisor Prof. Tadashi Matsumoto, who is full of enthusiasm in his academic life, has taught me a lot of things about research, as well as truth in life. I really appreciate his efforts to take me into a new exciting world. Without his guidance and encouragement, I could not have made those achievements shown in this thesis.

I am very appreciative to the assistance and valuable suggestions from Associate Professor Brian Michael Kurkoski. Deep thanks to Assistant Professor Khoirul Anwar who spent a lot of time to help me on research. Also, I am grateful to Professor Mineo Kaneko for the invaluable comments and kindly help.

I would like to take this opportunity to express my gratitude to all members of Information Theory and Signal Processing Laboratory for their great support and help in both daily life and academic research.

Here, I want to mourned with deep grief for one of our most honorable and excellent graduates Kisho Fukawa, who passed away recently. His developed Extrinsic Information Transfer (EXIT)-constrained Switching Algorithm (EBSA) which can optimize the coding chain effectively, is alive forever, and his spirit always in our mind. May he rest in Peace.

I wish to thank Hitachi Kokusai Electric Inc. for their financial support. Many thanks to Mr. Kobayasi and other members of Hitachi Kokusai Electric Inc. for their insightful options on my research.

Finally, I would like to express my deepest thanks to my parents far in my homeland. I wish they can accept my apologies for I can not fulfil my filial duty at their side. Also I want to thank my wife for her always support and encouragement. Without her love and understanding, this thesis could not reached the current quality level.

Abstract

In this thesis, the outage probabilities of correlated sources transmission systems are analyzed. The primary goal of this work is to derive theoretical limit for correlated sources transmission which utilize the source correlation, and to establish theoretical bases for wireless cooperative communications system design utilizing the correlated sources transmission concept. We focus on the problems that correlated sources are transmitted via channels having different statistical properties, and analyze how significant influent the differences of the statistical channel characteristics makes on the system outage.

First of all, in this thesis, the outage probability of a system having two correlated sources transmitted to common destination through Rayleigh and Rician fading channels is derived. The outage probability can be expressed by double integrals with respect to the probability density functions (PDF) of the instantaneous signal-to-noise power ratios (SNRs) of each channel, where the range of the integration is determined by the Slepian-Wolf theorem. This work identify the effect of the Rician factor K on the outage probability, where the K factor denotes the average power ratio of the line-of-sight (LOS) component power-to-non-line-of-sight (NLOS) components. To verify the consistency between the theoretical and practical results, we apply the technique to a Slepian-Wolf correlated sources transmission system where bit-interleaved coded modulation with iterative detection (BICM-ID) scheme is used. Performance comparison between the theoretical outage and the frame-error-rate (FER) shows that FER curves exhibit the same tendency as the theoretical results.

Moreover, we investigate the optimal power allocation for minimizing the outage probability with the condition that the total transmit power of the two sources is kept constant. The analytical results show that, so far as two sources are not fully correlated, lower outage probability can not always be achieved by increasing the transmit power ratio allocated to the source which transmits the signal via the channel have LOS component.

We then investigate the outage probability of a system having two correlated sources transmitted to common destination via Rayleigh and Nakagami-m fading channels, where the Nakagami-m fading channel model is known to more accurately represent the distribution of fading variations of the channel having LOS component than Rician fading channel model. The Nakagami-m distribution well represents the channel variations because it is derived from the measurement data gathered in real fields. The same analytical techniques as the one that are used in the Rician fading case is applied to calculate the

outage probability. The most significant contribution of this work is the derivation of a close-form expression for outage probability in several extreme cases. Furthermore, the asymptotic decay of the outage curves are derived theoretically.

In the main body of this thesis, we analyze the outage probability of a Slepian-Wolf correlated sources transmission system over Rayleigh and Rician fading channels, as well as over Rayleigh and Nakagami-m fading channels, respectively. Rician fading model can well be approximated by the Nakagami-m fading model by adjusting the factor K in Rician fading model and the factor m in Nakagami-m fading model. Hence, it is quite meaningful to identify the impact difference on outage performance. We investigate Kullback-Leibler distance (KLD), which is a measure of the difference between two probability distributions, between the Rician and Nakagami-m distributions. We then evaluated the impact of the KLD on the outage performance.

Keywords: Outage Probability, Rayleigh fading, Rician fading, Nakagami-m fading, Slepian-Wolf theorem, optimal power allocation, frame-error-rate (FER), bit-interleaved coded modulation with iterative detection (BICM-ID), LLR updating function, Kullback-Leibler distance (KLD)

Dedicated to my family

Contents

List of Figures

List of Tables

Chapter 1

Introduction

1.1 Background and Motivation

Cooperative communications, recognized as being one of the most important techniques in designing power-and-spectrally-efficient wireless communication networks, have been proposed and studied intensively in the last several years. In cooperative communications scenarios, nodes (i.e., base stations, mobile devices, stationary devices) form *virtual antenna array* [1] to cooperate with each other for better overall network performance, without requiring strict constraints in deployment or high hardware complexity, compared with *fixed* multiple-input multiple-output (MIMO) techniques [2].

Our research team has been focusing on creating of new concepts and technologies for next generation wireless communication systems, including this very hot topic. The most outstanding achievement made by our team is that the network, in general, can be seen as distributed coding system, as a whole, even though some of the nodes contain errors. Some valuable results achieved based on the considerations, have proven that these techniques can significantly improve performances of the wireless cooperative communication networks compared to the conventional technologies.

A simple three node cooperative transmission system is shown in Fig. 1.1, where the role of the destination (D) is to reconstruct the information transmitted from source 1 (S_1), with the help of information transmitted from source 2 (S_2). The destination receives two sequences, one from the S_1 and the other from the S_2. S_1 and S_2 can be seen as two sensors, for example, which are located near each other observing the same target, hence the information of S_1 and S_2 are correlated with each other. One can easily find that the relaying is straightforward application of the this transmission systems and the correlation between S_1 and S_2 can be regarded as source-relay link (intra-link) error

in relaying system. With the technique shown in [3–6], the Slepian-Wolf theorem [7] is applied to exploit the correlation knowledge between the information sequences sent from two sources. Hence it exemplifies a Slepian-Wolf correlated sources transmission system.

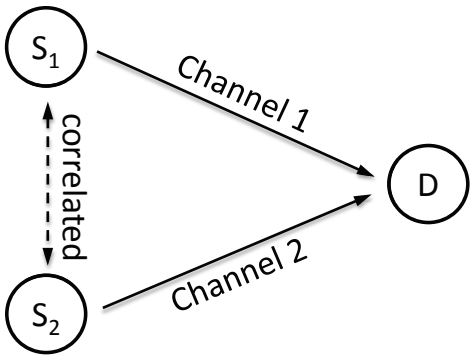

Figure 1.1: Diagrammatic sketch of correlated sources transmission system.

The relationship between the Slepian-Wolf correlated sources transmission and the relaying has been exploited in various ways. Information theoretic outage probability bound is derived in [3–5] and the optimal relay location is evaluated in [4]. A practical, simple coding and its iterative decoding technique are proposed by [6]. It is then further extended to the correlated sources transmission over multiple access channel (MAC) [8].

The results achieved by the previous research are all based on the assumption that the variations of the links all follow the Rayleigh distribution which is composed of only non-line-of-sight (NLOS) components. The impact of the line-of-sight (LOS) component is not considered. However, in real transmission environment, either the Channel 1 connecting S_1 to D or Channel 2 connecting S_2 to D, or the both, are often suffer from fading variation having different statistical properties. In relay systems, it is quite reasonable to assume that the Channel 2 has LOS component, resulting in the channel being Rician distributed. Moreover, we extend the problem to more generic and practical case, where fading variation follows the Nakagami-m distribution which is an empirically derived distribution through measurement data gathered in real fields [9].

This thesis investigates the outage probability of two correlated binary sources transmission, one via severe fading channel represented by Rayleigh fading, and the other via the channel with relatively mild fading represented by Rician or Nakagami-m distributions. The complex fading envelop is assumed to be constant over one transmission block, but vary block-by-block. This model is known as block fading model. We assume the correlation parameter between two sources is a constant over one block duration. In this thesis, we do not consider any practical transmission chain between two sources, and

only focus on two correlated source transmission. A series of simulations are conducted assuming a practical correlated sources transmission system to verify the performance tendencies. The objective of this work is to evaluate the impact of the mild fading channel on the transmission outage probability of the correlated sources transmission system, and to derive the theoretical limit of diversity and coding gains. Furthermore, this thesis investigates the optimal power allocation for minimizing the outage probability with keeping the total transmit power constant.

Since the Rician fading model can well be approximated by the Nakagami-m fading model, by adjusting the factor K in Rician fading model and the factor m in Nakagami-m fading model. The impact of the different statistical characteristics of the Rician and Nakagami-m fading variation on outage performance is evaluated, based on analysis of Kullback-Leibler distance (KLD), which is used to measure the difference between probability distributions.

1.2 Author's Contribution

This research derives the outage probability bound of two correlated sources transmission systems, and identifies the effect of LOS component in Rician fading channel on the outage probability. It is found that even through the significant reduction of the outage probability can be achieved with the help of the LOS component at a relatively low signal-to-noise power ratio (SNR) region, the diversity order exhibited in the outage curve asymptotically converges into one if the sequences of two sources are not fully correlated. Interestingly, although the asymptotic behaviour of the outage probability found in this work is the same as that shown in [3], the decay of the outage curve at the relatively low SNR value region is different, and the decay depending on the ratio of LOS-to-NLOS components. When two sources are fully correlated, the outage curves exhibit sharper decay than that with the $2nd$ order diversity in the presence of the LOS component of the Rician channel. To verify the accuracy of the theoretical results, we apply the Slepian-Wolf correlated sources transmission technique presented in [6] to a bit-interleaved coded modulation with iterative detection (BICM-ID) scheme [10, 11]. Performance comparison between the theoretical outage and the frame-error-rate (FER) performance clearly shows that FER curves exhibit the same tendency as the theoretical results. Furthermore, optimal power allocation for minimizing the outage probability is investigated with the condition that the total transmit power of two sources is kept constant. The optimal power allocation largely depends on the ratio of the LOS-to-NLOS components when two

sources are fully correlated. Surprisingly, if two sources are not fully correlated, increasing the ratio of transmit power, allocated to signal transmitted via the Rician channel, does not always improve the outage performance.

Also, we investigate the outage probability of two correlated sources transmitted to common destination via the Rayleigh and Nakagami-m fading channels, where the Nakagami-m distribution is know to be more accurately represent the channel behaviour in the presence of LOS component than the Rician fading channel model, in terms of the $1st$ order statistics, because it was derived from the measurement data gathered in real fields. The most significant contribution of this part of the work is the derivation of the closed-form expression for the outage probability in several extreme cases. Furthermore, the asymptotic decay of the outage curves are analyzed theoretically.

It can be found from the previous work that, although Rician fading model can well be approximated by the Nakagami-m fading model, by adjusting the factor K in Rician fading model and the factor m in Nakagami-m fading model, the outage performances of Slepian-Wolf correlated sources transmission systems over Rician and Nakagami-m fading channels are not identical to each other. We analyze the reason for the different tendency by calculating the KLD between of Rician and Nakagami-m distributions having the corresponding K and m factors. The impact of the KLD on outage performance is also investigated. The results clearly indicate the theoretical limit for designing and/or evaluating the techniques for relaying system of which some of the coverage have LOS propagation components.

1.3 Thesis Organization

This thesis is organized as follows:

In **chapter 2**, we provide the definitions of some terminological bases used in this thesis, and introduce knowledge background of this thesis, including different type of fading channel, fundamental concept of diversity, LOS and NLOS channels and Slepian-Wolf Theorem.

Chapter 3 focuses on two correlated sources transmission over Rayleigh and Rician fading channels. In this chapter, the definition and the derivation of the outage probability are presented, and their asymptotic tendency analysis as well. The accuracy of the theoretical analyses are verified through the simulations for the Slepian-Wolf correlated sources transmission system based on BICM-ID technique. The last part of this chapter is devoted to the optimal power allocation problem for minimizing the outage probability

with the condition that the total transmit power of two sources is kept constant.

Chapter 4 investigates the problem of correlated sources transmission over Rayleigh and Nakagami-m fading channels. The closed-form expression for outage probability in several extreme cases are derived. Moreover, the asymptotic decay of the outage curves are derived theoretically. The consistency between the theoretical analysis results and FER performances are verified through computer simulations conducted assuming practical yet simple relay system.

Chapter 5 calculates KLD between of Rician and Nakagami-m distribution and investigates the impact of the distributions difference on outage performance obtained from **chapter 2** and **chapter 3**.

Chapter 6 summarizes this thesis and outline the issues left as future research.

- It should be emphasized that some of the mathematical expressions/formulas are found by this thesis for the first time in the communication research community.

Chapter 2

Definitions and Knowledge Background

In this chapter, we present the concept of the technique investigated in this thesis, and introduce background knowledge that forms the technological bases of this thesis. First, we introduce the concept of LOS and NLOS channels. We then describe the characteristics of the fading channels investigated in this thesis, namely, the Rayleigh, Rician, and Nakagami-m fading channels. The relationship between of diversity order and the decay of and bit-error-rate (BER) curve is presented. Finally, we briefly introduce the Slepian-Wolf theorem which defines theoretical bound of the rate for lossless distributed sources coding.

2.1 LOS and NLOS

In wireless communications, assuming there are no obstacles in the free space between the transmitter and the receiver, and the signal propagates along a straight line between them. The model associated with this transmission is called LOS channel model, and the corresponding received signal is called LOS signal or LOS component. On the contrary, if there are obstacles between the transmitter and the receiver, and hence there are no LOS components in the received signal, it is referred to as NLOS channel. In practice, the deep space probe and aircraft-to-aircraft communications can be considered as LOS channel transmission. In many of the terrestrial communications system, such as WiFi, and mobile communication systems, the channels have LOS plus NLOS components.

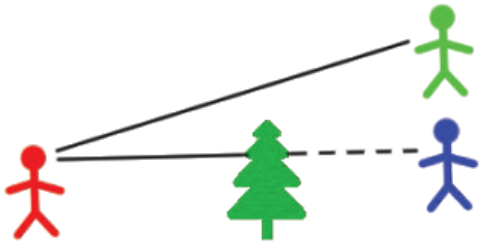

Figure 2.1: LOS vs NLOS channel

2.2 Fading Channels

In wireless communications, if the transmitter or the receiver, or the both, moves/move, the channel's complex envelope vary, and hence the channel becomes time-varying random processes. In this scenario, the channel suffers from fading.

Rayleigh Fading Channel

- Rayleigh fading channel is a communication channel composed of NLOS components only, and the channel variation fallows Rayleigh distribution. Rayleigh fading model is most widely used when there is no dominant propagation path between the transmitter and the receiver; it is composed of NLOS components only. If there are sufficient scatters in the environment, all the reflected signals that arrive at the reviver form a received composite single, of which equivalent baseband complex envelope follows two-dimensional Gaussian distribution. Its phase and amplitude are statistically independent, and the in-phase (I) and quadrature (Q) components (the real and imaginary parts of the equivalent baseband complex envelope, respectively), X and Y, respectively, follows independent Gaussian distribution. Hence, with the two zero mean Gaussian variables X and Y with equal variance σ^2, the amplitude Z of the complex envelope

$$Z = \sqrt{X^2 + Y^2} \tag{2.1}$$

  follows Rayleigh distribution [9].

Rician Fading Channel

- As stated in section 2.1, in many of the terrestrial communications system, the channel is composed of LOS and NLOS components. A mathematical model of the channel having LOS and NLOS components is Rician fading channel, where

the amplitude is characterized by a Rician distribution. The Rician fading model widely used to the channels that exploit the performance gain due to the LOS conditions. The composite NLOS component is modelled as zero-mean complex Gaussian random variable. Consider two Gaussian random variables $X^{'}$ and $Y^{'}$, both having the same variance σ^2. $X^{'}$ has non-zero mean which corresponds to the amplitude of the LOS component, while $Y^{'}$ has zero mean. Then, the signal amplitude $Z^{'}$ defined as

$$Z^{'} = \sqrt{X^{'2} + Y^{'2}}, \tag{2.2}$$

follows Rician distribution. Rayleigh fading can be considered as a special case of Rician fading where there is NLOS components, i.e, the mean of $X^{'}$ is zero.

Nakagami-m Fading Channel

- Although the Rician distributions are widely used to represent the statistical behaviors of the channels, however, they are still not accurate enough, when the $1st$ order statistics of the channel variations is compared with the measurement data gathered in real fields. The Nakagami-m distribution is derived empirically based on the measurement data, and is known as being able to better represent the distribution of the channel behaviours compared to the Rician distribution [12]. Both Rayleigh and Rician distributions are connected by a factor of the Nakagami-m distribution.[13].

2.3 Diversity

Diversity is a well-know technique for improving the performances of wireless communications in fading channels. Independently varying paths in the propagation process achieves diversity gains. The main advantage of the receive diversity is that it mitigates the signal fluctuations due to fading. The diversity order indicates the decay of the slope of BER or FER curves as a function of the average SNR.

As shown in Fig. 2.2, with the $1st$ order diversity (no diversity), increasing average SNR by 10 dB, average BER can be reduced by one decade. When the diversity order increases, the better BER performance can be achieved at the same average SNR point.

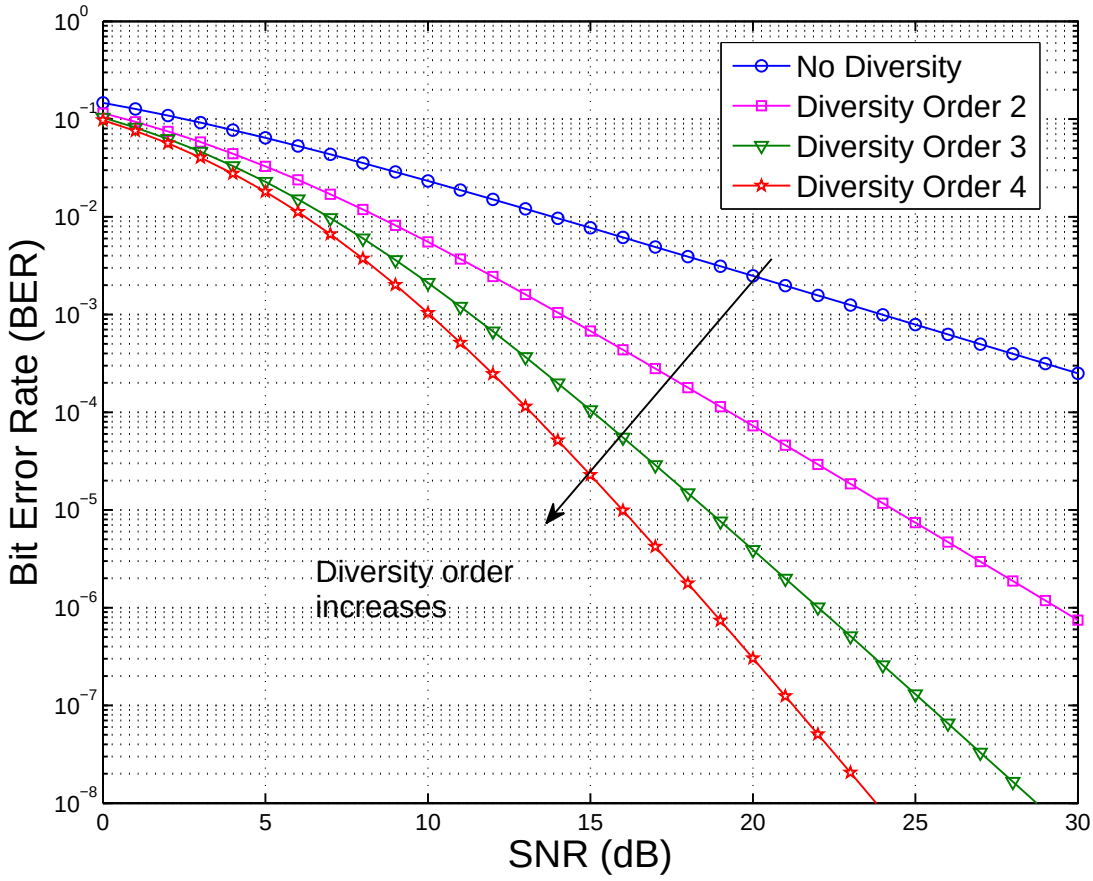

Figure 2.2: Diversity order

2.4 Slepian-Wolf Theorem

In single source transmission, if the source information is compressed to a rate which is not smaller than its entropy, the source information can be reconstructed with arbitrary small error probability at the destination. This have been proved by Cloud Shannon in his landmark paper [14]. According Sleipin and Wolf's outstanding contribution in [7], for two correlated sources, if the rate of each source allocated after compression is not smaller than its conditional entropy and if the sum rate is not smaller than the two source's joint entropy, still the source information can be recovered losslessly. More explicitly, source rate R_{S1} and R_{S2} must satisfy the three inequalities:

$$R_{S1} \geq H(\mathbf{b}_1|\mathbf{b}_2), \tag{2.3}$$

$$R_{S2} \geq H(\mathbf{b}_2|\mathbf{b}_1), \tag{2.4}$$

$$R_{S1} + R_{S2} \geq H(\mathbf{b}_1, \mathbf{b}_2), \tag{2.5}$$

where $H(\cdot|\cdot)$ and $H(\cdot,\cdot)$ denote the conditional and the joint entropy, respectively. The admissible rate region is specified as shown in Fig. 2.3. So far as the rate pair (R_{S1}, R_{S2}) falls into the admissible rate region, the error probability can be made arbitrarily small when recovering the transmitted information at the destination.

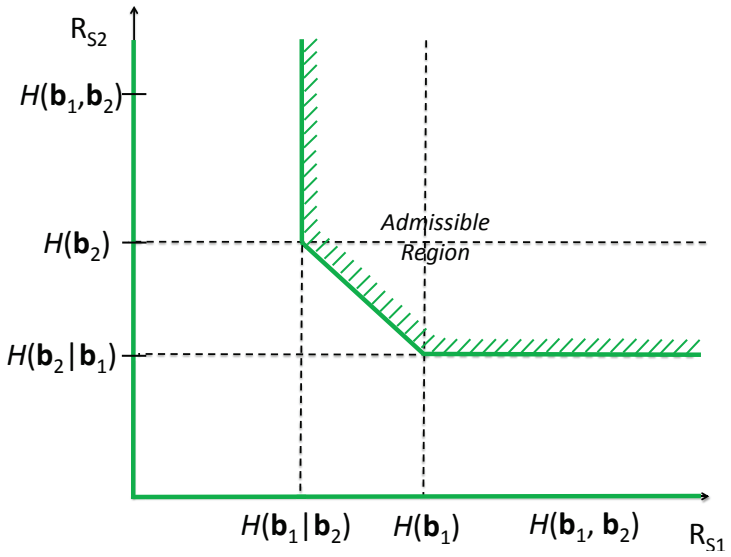

Figure 2.3: The admissible rate region of Slepian-Wolf theorem.

Chapter 3

Correlated Sources Transmission over Rician fading Channels

In this chapter, outage probability of a Slepian-Wolf correlated sources transmission system is analyzed. The achievable outage bound is derived theoretically. We consider two correlated binary information sequences following *bit-flipping* model [15], where the information bits of the second source are a *flipped* version of the information bits of the first source, with a certain flipping probability. The information sequence of one source is transmitted over Rayleigh fading channel, while information sequence of the other source is transmitted over Rician fading channel. We derive mathematical expression for the outage probability, which can be evaluated by employing a numerical technique. The theoretical asymptotic tendency of the outage probability performance is analyzed. Finally, simulations for the Slepian-Wolf correlated sources transmission system are conducted to verify the consistency between the theoretical outage and FER curves, assuming a practical yet simple relay system.

3.1 System Model

3.1.1 Bit-flipping Model

In this thesis, we use *bit-flipping* model to represent the correlation between the sources, to be transmitted over the cooperative communications system. The correlation is modelled by $\mathbf{b}_2 = \mathbf{b}_1 \oplus \mathbf{e}$, where $\mathbf{b}_1$ and $\mathbf{b}_2$ are two binary information sequences taking value from $\{0, 1\}$, and $\mathbf{e}$ is a random variable which take value 1 with probability p_f and value 0 with probability $1 - p_f$, i.e., $\Pr(e = 1) = p_f$ [15]. Hence, the correlation between the

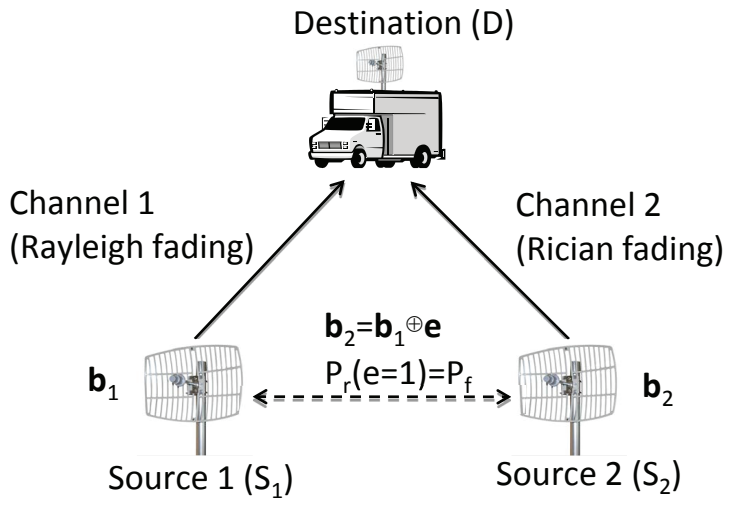

Figure 3.1: System model for Slepian-Wolf correlated sources transmission system: different fading channel scenarios.

two sources is given by $\rho = 1 - 2p_f$, meaning that the information bits of the $\mathbf{b}_2$ are a *flipped* version of the information bits of $\mathbf{b}_1$, with a probability p_f.

3.1.2 Slepian-Wolf Correlated Sources Transmission System

The system model we use to analyze the correlated sources transmission is shown in Fig. 3.1. $\mathbf{b}_1$ and $\mathbf{b}_2$ are the correlated information bit sequence to be sent from source 1 (S_1) and source 2 (S_2) to the common destination (D), via Channel 1 and Channel 2, respectively. Channel 1 is suffering from block Rayleigh fading whereas Channel 2 from block Rician fading. In block fading channel, channel gain is constant within a block, but change block-by-block and link-by-link, following the distribution. The information bit sequence $\mathbf{b}_1$ is transmitted from S_1 through Channel 1 during the first time slot, then the information bit sequence $\mathbf{b}_2$ is transmitted from the S_2 through Channel 2 during the second slot, hence the transmission is orthogonal.

3.2 Outage Probability Derivation

3.2.1 Outage Probability under Fading

Outage probability is a measure of the quality of the transmission over mobile wireless communication channels. In fading channels, transmitted signal may suffer from deep fades, resulting in a loss (outage) of the signal. Outage occurs when the received instan-

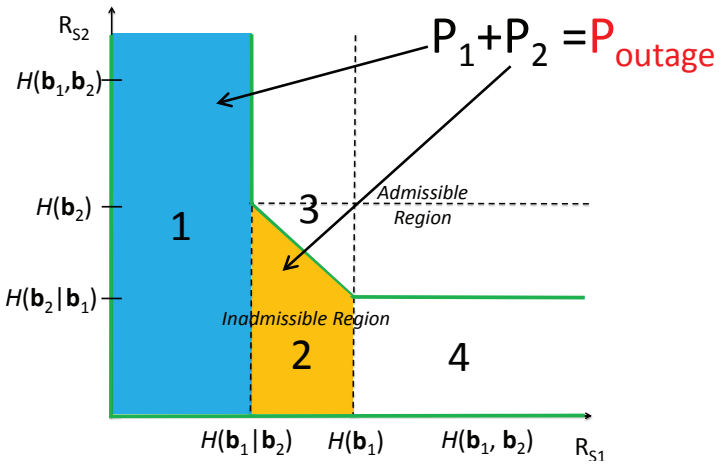

Figure 3.2: Outage definition based on Slepian-Wolf correlated sources transmission system.

taneous SNR γ is below a certain threshold lever γ_s. Therefore, the outage probability is defined as

$$P_{out} = Pr(\gamma < \gamma_s) = \int_0^{\gamma_s} p_\gamma(\gamma) d\gamma \tag{3.1}$$

where $p_\gamma(\gamma)$ is probability density function (PDF) of the instantaneous SNR.

3.2.2 Outage Probability Definition for Slepian-Wolf Correlated Sources Transmission System

The set of Slepian-Wolf rate pair (R_{s1}, R_{s2}) shown in Fig. 3.2 is divided into two regions, the admissible and inadmissible regions. If rate pair (R_{s1}, R_{s2}) falls into the inadmissible region, the transmission outage event occurs and the decoder at the destination can not guarantee the reconstruction of the original information with arbitrarily small error probability. Furthermore, the inadmissible region can be divided into three areas 1, 2, and 4 as shown in Fig. 3.2. In this thesis, we consider the case where $\mathbf{b}_2$ transmitted from S_2 is the copy of $\mathbf{b}_1$ transmitted from of S_1 with some *flipped* bits, and only $\mathbf{b}_1$ needs to be recovered. We focus on analyzing the impact of $\mathbf{b}_2$ transmitted through Channel 2 on the outage probability. Therefore, an arbitrary value of R_{s2} is acceptable so long as R_{s1} is larger than $H(\mathbf{b}_1)$. Hence, the area 4 in Fig. 3.2 can also be included in the admissible rate region. Hence, the outage probability of the system model we consider

can be expressed as

$$P_{\text{outage}} = P_1 + P_2, \tag{3.2}$$

where P_1 and P_2 denote the probabilities that the rate pair R_{s1}, R_{s2} fall into the inadmissible area 1 and area 2, respectively. Hence, outage analysis turns to be the probability calculation of R_{s1} and R_{s2} falling into the unbounded rectangular area 1 and the trapezoidal area 2 shown in Fig. 3.2. Thus, the conditions on R_{s1} and R_{s2} that can not guarantee arbitrary low bit error rate transmission are given by

$$P_1 = \Pr\left[0 < R_{\text{s1}} < H(\mathbf{b}_1|\mathbf{b}_2), R_{\text{s2}} > 0\right] \tag{3.3}$$

$$P_2 = \Pr\left[H(\mathbf{b}_1|\mathbf{b}_2) < R_{s1} < H(\mathbf{b}_1), R_{\text{s1}} + R_{\text{s2}} < H(\mathbf{b}_1, \mathbf{b}_2)\right], \tag{3.4}$$

where R_{c1} and R_{c2} represent the spectrum efficiencies of the transmission chain, including the channel coding scheme and modulation multiplicity within Channel 1 and Channel 2, respectively.

According to Shannon's separation theorem [14], if the total information transmission rate satisfies

$$R_s \cdot R_c \leq C, \tag{3.5}$$

the error probability can be reduced to arbitrarily low at the destination, where R_s and R_c denote the rates after source and channel coding, including the modulation multiplicity, respectively. C is the channel capacity. When Gaussian codebook is used, C can be given by

$$C = \log_2\left(1 + \gamma\right), \tag{3.6}$$

Assume the channel code used is capacity-achieving,

$$R_s \cdot R_c = C. \tag{3.7}$$

According to (3.6) and (3.7), the relationship between the threshold instantaneous SNR γ_s and its corresponding source coding rate R_s is given by

$$R_s = \frac{1}{R_c}\log_2(1 + \gamma_s). \tag{3.8}$$

Since, we assumed that the Source-Channel separation holds [16], R_c can be independent of R_s.

By utilizing the relationship 3.8 to 3.3 and 3.4, outage probability can be rewritten as

$$P_1 = \Pr\left[0 < \gamma_1 < 2^{R_{c1}H(\mathbf{b}_1,\mathbf{b}_2)} - 1, \gamma_2 > 0\right], \tag{3.9}$$

$$P_2 = \Pr\left[2^{R_{c2}H(\mathbf{b}_1|\mathbf{b}_2)} - 1 < \gamma_1 < 2^{R_{c1}H(\mathbf{b}_1)} - 1, 0 < \gamma_2 < 2^{\left[R_{c2}H(\mathbf{b}_1,\mathbf{b}_2) - \frac{R_{c2}}{R_{c1}} log_2(1+\gamma_1)\right]} - 1\right]. \tag{3.10}$$

which can be used for outage probability calculation based on the PDF with instantaneous SNRs of Channel 1 and Channel 2.

3.2.3 Outage Calculation for Slepian-Wolf Correlated Sources Transmission System

With the assumption that Channel 1 suffers from block Rayleigh fading, the PDF with instantaneous SNR γ_1 of Channel 1 is given by

$$p(\gamma_1) = \frac{1}{\overline{\gamma}_1} \exp(-\frac{\gamma_1}{\overline{\gamma}_1}), \tag{3.11}$$

where $\overline{\gamma}_1$ represents the average SNR of Channel 1. Channel 2 is assumed to suffer from block Rician fading, of which variation is independent of Channel 1. The PDF with instantaneous SNR γ_2 of Channel 2 is given by

$$p\left(\gamma_2\right) = \left(\frac{\left(1+K\right)e^{-K}}{\overline{\gamma}_2}\right) \exp\left(-\frac{(1+K)\gamma_2}{\overline{\gamma}_2}\right) \cdot I_0\left(2\sqrt{\frac{K\left(1+K\right)\gamma_2}{\overline{\gamma}_2}}\right), \tag{3.12}$$

where $I_0(\cdot)$ is the zero-th order modified Bessel function of the first kind and $\overline{\gamma}_2$ is the average SNR of Channel 2. The Rician factor K in (3.12) is the power ratio of the LOS component-to-the power of the NLOS multipath components [9]. K represents the severity of fading. With $K = \infty$, the channel is equivalent to a static additive white Gaussian noise (AWGN) channel, and with $K = 0$ the channel reduces to Rayleigh fading channel.

Based on (3.9), (3.10), (3.11) and (3.12), the outage probability P_1 in can then be

mathematically expressed as

$$\begin{aligned} P_1 &= \int_{\gamma_1=0}^{2^{R_{c1}H(\mathbf{b}_1|\mathbf{b}_2)}-1} p(\gamma_1)d\gamma_1 \int_{\gamma_2=0}^{\infty} p(\gamma_2)d\gamma_2 \\ &= \int_{\gamma_1=0}^{2^{R_{c1}H(\mathbf{b}_1|\mathbf{b}_2)}-1} \frac{1}{\overline{\gamma}_1}\exp(-\frac{\gamma_1}{\overline{\gamma}_1})d\gamma_1 \\ &= 1-\exp\left(-\frac{2^{R_{c1}H(\mathbf{b}_1|\mathbf{b}_2)}-1}{\overline{\gamma}_1}\right), \end{aligned} \tag{3.13}$$

according to the assumption that Channel 1 and Channel 2 are statistically independent. By introducing the cumulative density function (CDF) of Rician fading channel, P_2 can be calculated as

$$\begin{aligned} P_2 &= \int_{\gamma_1=2^{R_{c1}H(\mathbf{b}_1|\mathbf{b}_2)}-1}^{2^{R_{c1}H(\mathbf{b}_1)}-1} p(\gamma_1) \int_{\gamma_2=0}^{2^{\left[R_{c2}H(\mathbf{b}_1,\mathbf{b}_2)-\frac{R_{c2}}{R_{c1}}\log_2(1+\gamma_1)\right]}-1} p(\gamma_2)d\gamma_2 d\gamma_1 \\ &= \int_{\gamma_1=2^{R_{c1}H(\mathbf{b}_1|\mathbf{b}_2)}-1}^{2^{R_{c1}H(\mathbf{b}_1)}-1} p(\gamma_1)\left[1-Q_1\left(\sqrt{2K},\sqrt{2\left(1+K\right)\frac{\gamma_2}{\overline{\gamma}_2}}\right)\right]_{\gamma_2=0}^{2^{\left[R_{c2}H(\mathbf{b}_1,\mathbf{b}_2)-\frac{R_{c2}}{R_{c1}}\log_2(1+\gamma_1)\right]}-1} d\gamma_1 \\ &= \int_{\gamma_1=2^{R_{c1}H(\mathbf{b}_1|\mathbf{b}_2)}-1}^{2^{R_{c1}H(\mathbf{b}_1)}-1} \frac{1}{\overline{\gamma}_1}\exp\left(\frac{-\gamma_1}{\overline{\gamma}_1}\right)\left[1-Q_1\left(\sqrt{2K},\sqrt{\frac{\left(1+K\right)2^{\left[R_{c2}H(\mathbf{b}_1,\mathbf{b}_2)-\frac{R_{c2}}{R_{c1}}\log_2(1+\gamma_1)\right]}}{\overline{\gamma}_2}}\right)\right] d\gamma_1, \end{aligned} \tag{3.14}$$

where $Q_1(\cdot,\cdot)$ is the Marcum Q-Function. The derivation of an explicit expression of P_2 given by (3.14) may be intractably complicated. Hence, the recursive adaptive Simpson quadrature algorithm [17] is used to approximate the integral of (3.14), with accurate calculation error control.

3.3 Asymptotic Tendency Analysis

Since the binary symmetric source model is assumed in this work,

$$H(\mathbf{b}_1) = H(\mathbf{b}_2) = 1, \tag{3.15}$$

$$H(\mathbf{b}_1|\mathbf{b}_2) = H(\mathbf{b}_2|\mathbf{b}_1) = H(p_f), \tag{3.16}$$

$$H(\mathbf{b}_1,\mathbf{b}_2) = 1 + H(p_f), \tag{3.17}$$

where $H(p_f) = -p_f\log_2(p_f) - (1-p_f)\log_2(1-p_f)$.

3.3.1 Tendency 1: Independent Sources Case

When $\mathbf{b}_1$ and $\mathbf{b}_2$ are independent ($p_f = 0.5$), $H(\mathbf{b}_1|\mathbf{b}_2) = H(\mathbf{b}_1)$. In this case, the range of the integral with respect to γ_1 in (3.14) is from 0 to 0. Hence, the probability P_2 equals to 0. Consequently, the outage probability is entirely dominated by P_1, i.e., P_{out}=P_1. Moreover, since $\mathbf{b}_1$ and $\mathbf{b}_2$ are completely uncorrelated, $H(\mathbf{b}_1|\mathbf{b}_2) = H(\mathbf{b}_2|\mathbf{b}_1) = 1$. Therefore, P_1 are just the same as the outage probability of single Rayleigh channel's case, as

$$P_{\text{out,Rayleigh}} = 1 - \exp\left(-\frac{2^{R_{c1}} - 1}{\overline{\gamma}_1}\right), \tag{3.18}$$

which corresponds to the $1st$ order diversity.

3.3.2 Tendency 2: Large Average SNR Case

When average SNR $\overline{\gamma}_1 \to \infty$ and $\overline{\gamma}_2 \to \infty$, the outage probability $P_2 \to 0$ because the Marcum Q-Funcion in (3.14) approaches 1 as the second term of Marcum Q-Funcion becomes small. Therefore, only P_1 dominates the outage probability in this case. Furthermore P_1 can be rewritten by the Taylor expansion, as

$$P_1 = \sum_{n=0}^{\infty} \frac{(-1)^{(n)}}{n+1!} \left(\frac{2^{R_{c1}H(\mathbf{b}_1|\mathbf{b}_2)} - 1}{\overline{\gamma}_1}\right)^{n+1}. \tag{3.19}$$

However, the (3.19) has domination of first term when $\overline{\gamma}_1$ is large. Thus, (3.19) can be approximated, as

$$P_1 \approx \frac{2^{R_{c1}H(\mathbf{b}_1|\mathbf{b}_2)} - 1}{\overline{\gamma}_1}, \tag{3.20}$$

which follows the tendency of the $1st$ order diversity. Interestingly, this observation indicates that outage performance is determined by the NLOS components when the average SNRs $\overline{\gamma}_1$ and $\overline{\gamma}_2$ become large.

3.3.3 Tendency 3: Fully Correlated Sources Case

When $\mathbf{b}_1$ and $\mathbf{b}_2$ are fully correlated ($p_f = 0$), the conditional entropy $H(\mathbf{b}_1|\mathbf{b}_2) = 0$. Therefore, the probability P_1 is equals to 0, according to (3.13). Hence, the outage probability is completely dominated by P_2, i.e., P_{out}=P_2. The results of the numerical integral for (3.14) is shown in Fig. 3.3. It is found that the outage curves decay is sharper than the $2nd$ order diversity when the K factor becomes large.

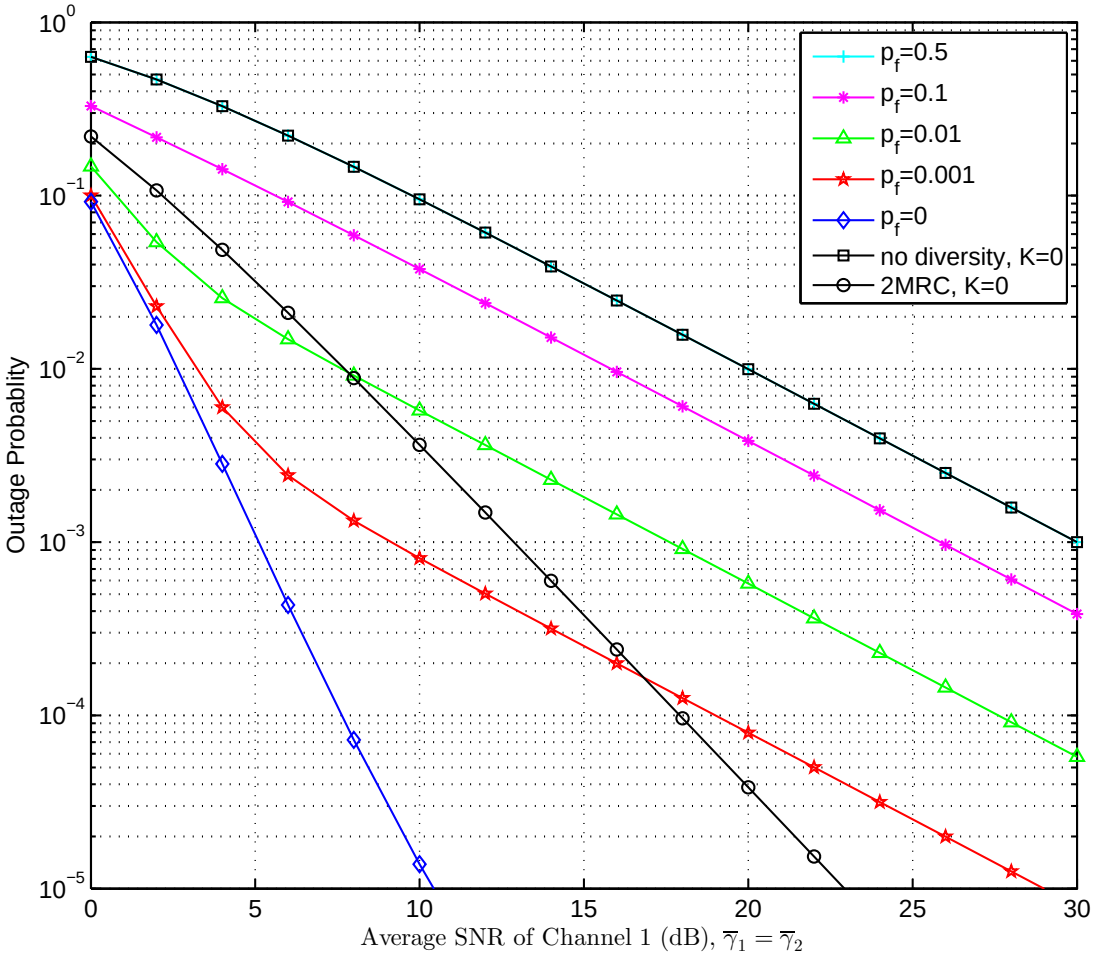

Figure 3.3: Outage probability with different p_f for $K = 10$.

However, for the case $K = 0$, with which Rician fading reduces to Rayleigh, according to the the property of Marcum Q-function

$$Q_1(0, b) = \exp\left(-\frac{b^2}{2}\right). \tag{3.21}$$

By assuming that the fading variation of the two channels are statistically independent and the spectrum efficiency of the transmission chain representing the coding rate and the multiplicity of the modulation for both channels are equal to one, i.e., R_{c1}=R_{c2}=1, P_2 is reduced to

$$\begin{aligned} P_2 &= \int_{\gamma_1=0}^{1} p(\gamma_1) \int_{\gamma_2=0}^{2^{[1-\log_2(1+\gamma_1)]}-1} p(\gamma_2) d\gamma_2 d\gamma_1 \\ &= \int_0^1 p(\gamma_1) \left[1 - Q_1\left(0, \sqrt{\frac{2\gamma_2}{\overline{\gamma}_2}}\right)\right]_{\gamma_2=0}^{2^{[1-\log_2(1+\gamma_1)]}-1} d\gamma_1 \\ &= \frac{1}{\overline{\gamma}_1} \int_0^1 \left[\exp(-\frac{\gamma_1}{\overline{\gamma}_1}) - \exp\left(-\frac{\gamma_1}{\overline{\gamma}_1} + \frac{1}{\overline{\gamma}_2} - \frac{2}{\overline{\gamma}_2\,(1+\gamma_1)}\right)\right] d\gamma_1. \end{aligned} \tag{3.22}$$

According to the Taylor expansion, we have

$$\exp(-x) = \sum_{n=0}^{\infty} \frac{(-x)^n}{n!} \approx 1 - x, \ as \ x \to 0. \tag{3.23}$$

Then, (3.22) can be approximated as

$$\begin{aligned} P_2 \approx & \frac{1}{\overline{\gamma}_1} \int_0^1 \left[\left(1 - \frac{\gamma_1}{\overline{\gamma}_1}\right) - \left(1 - \frac{\gamma_1}{\overline{\gamma}_1} - \frac{1-\gamma_1}{\overline{\gamma}_2\,(1+\gamma_1)}\right)\right] d\gamma_1 \\ = & \frac{1}{\overline{\gamma}_1} \left[\frac{2\ln(1+\gamma_1) - \gamma_1}{\overline{\gamma}_2}\right]_0^1 \\ = & \frac{2\ln 2 - 1}{\overline{\gamma}_1 \overline{\gamma}_2}. \end{aligned} \tag{3.24}$$

It is obvious that P_2 (=P_{out}) is inversely proportion to the product of $\overline{\gamma}_1$ and $\overline{\gamma}_2$, and hence $2nd$ order diversity gain can be achieved when $p_f = 0$. This conclusion is consistent to the result of [5], where both source-destination (SD) and relay-destination (RD) channels are suffering from Rayleigh fading.

3.4 Numerical Results and Discussion

3.4.1 Equal Average SNR with Channel 1 and Channel 2

In Fig. 3.3, the theoretical outage probability versus average SNR are drawn with a parameter p_f varying from 0 to 0.5, assuming that average SNRs of Channel 1 and Channel 2 are identical, i.e., $\overline{\gamma}_1$=$\overline{\gamma}_2$, and K=10. It should be noticed that with the Rician factor $K = 10$, fading variation of Channel 2 is not as severe as that of Channel 1. The outage probability curves of maximum-ratio-combining (MRC) with p_f=0 and K=0 (Rayleigh), and that of no diversity are shown as reference curves. We can see that there is no diversity gain when $p_f = 0.5$, and the outage curve is exactly the same as that in Rayleigh fading without diversity. This is also consistent to the asymptotic tendency analysis result provided in the sub-section 3.3.1. It should be noticed that, the lower the p_f value, the smaller the outage probability. The outage probability can achieve sharper decay than with the $2nd$ order diversity if $\mathbf{b}_1$ and $\mathbf{b}_2$ are entirely correlated ($p_f = 0$). In this case, only P_2 dominates the outage probability. The results are consistent to the findings provided in sub-section 3.3.3.

Fig. 3.4 demonstrates the outage probability curves versus average SNR with the Rician factor K as a parameter, where the *bit-flipping* probability is fixed at $p_f = 0.001$, indicating that $\mathbf{b}_1$ and $\mathbf{b}_2$ are highly correlated, but $\mathbf{b}_2$ still contains some flipped bits. It is found that the outage curves exhibit the following tendencies; when the average SNR is small, the outage probability reduces quickly, however, the decay of the outage curves always asymptotically converges into the $1st$ order diversity when the $\overline{\gamma}_1$ and $\overline{\gamma}_2$ increases. This observation is also exactly consistent to the asymptotic tendency analysis conclusion provided in sub-section 3.3.2. Although the asymptotic behaviour is the same as that shown in [3] which assumes the both channels suffer from Rayleigh fading, the convergence to the asymptotic performance is not exactly the same, and it is depending on the energy of the LOS component of Channel 2. So far as $p_f \neq 0$, the outage probability curves always show the tendency described above.

3.4.2 Impact of Different Average SNR

In this sub-section, the outage probabilities are shown with the Rician factor K as a parameter. The difference from the previous sub-section is that the average SNRs of the two channels are not assumed to be identical. In Fig. 3.5, the outage probability curves are depicted, where $\overline{\gamma}_2 - \overline{\gamma}_1 = 10$ dB, and $p_f = 0.001$. P_1 is independent of the

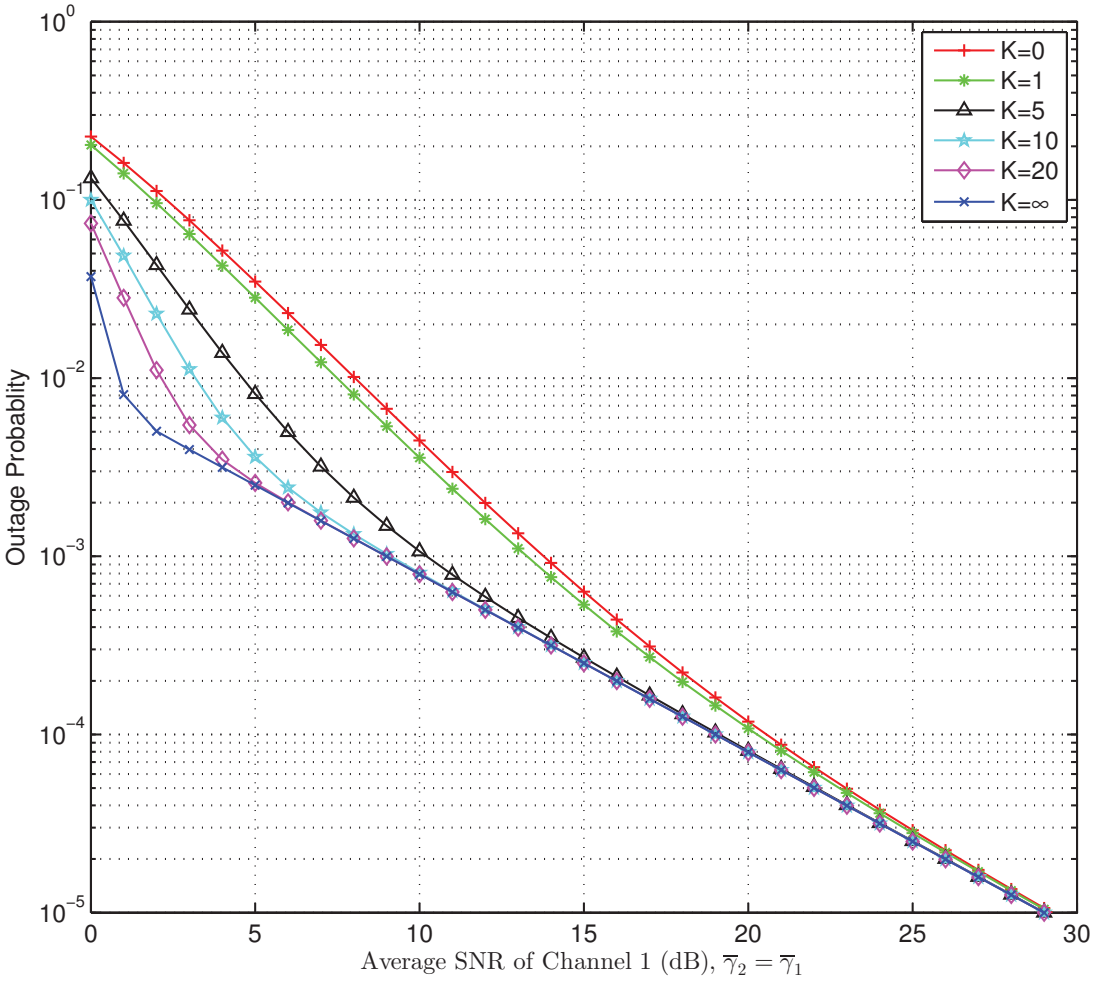

Figure 3.4: Outage probability with different K for $\overline{\gamma}_1 = \overline{\gamma}_2$.

K factor, according to (3.13), whereas P_2 is affected by K. The decay of outage curves asymptotically converge in to the $1st$ order diversity as the average SNR increases. It is also found from Fig. 3.4 and Fig. 3.5 that, when the average SNR is lower than the value at which the outage starts to converge to such asymptotic tendency, P_2 is dominated by the K factor. Hence, the turning point depends on difference between $\overline{\gamma}_1$ and $\overline{\gamma}_2$.

3.4.3 Consistency Verification between the Theoretical and Simulation Results for a Practical System

A. BICM-ID based Slepian-Wolf Correlated Sources Transmission System

In this sub-section, we introduce a BICM-ID based Slepian-Wolf correlated sources transmission System, and evaluate its FER performance. The purpose of the simulation is to verify the consistency between the FER performance and the theoretical outage results. The block diagrams of the system is shown in Fig. 3.6. The original information bits $\mathbf{b}_1$ of S_1 are channel-encoded by C_1 which is a rate-1/2 general polynomial (3,2) convolutional code. The channel coded bits output from C_1 are interleaved by interleaver π_1 and further fed into a doped accumulator ($DACC_1$). $DACC_1$ has the same structure as memory-1 half rate systematic recursive convolutional code (SRCC) with a doping ratio d [18]. The purpose of the use of $DACC$ is to keep the convergence tunnel in the extrinsic information transfer (EXIT) curve of the corresponding decoder $DACC^{-1}$ reaches a point very close to the (1,1) mutual information point [8]. Finally, the bit stream output from the $DACC_1$ is mapped onto symbol sequence $\mathbf{s}_1$ according to the specified mapping rule. Quaternary-phase-shift-keying (QPSK) is assumed in the simulation. $\mathbf{s}_1$ are transmitted to destination via Rayleigh fading channel during the first time slot. It should be noticed that because of use of rate-1/2 channel coding and QPSK modulation, the spectrum efficiency R_{c1} representing channel coding rate and modulation multiplicity of the transmission chain is equal to one.

As denoted before, $\mathbf{b}_2$ is a copy of information bits $\mathbf{b}_1$ with a *bit-flipping* probability p_f. $\mathbf{b}_2$ is channel-coded by C_2 and interleaved by the interleaver π_2. The interleaved bits are fed into $DACC_2$, in the same way as that for $\mathbf{b}_1$, and then modulated with a specified mapping rule to generate the symbol sequence $\mathbf{s}_2$. Finally, the symbol sequence $\mathbf{s}_2$ are transmitted to the common destination via Rician fading channel during second time slot.

At the destination, the demapper calculates the extrinsic log-likelihood ratio (LLR) of information bits $L_e(b_1)$ composing $\mathbf{s}_1$, and $L_e(b_2)$ composing $\mathbf{s}_2$, respectively, based on the BICM-ID principle [19]. With the help of a priori LLR information $L_a(b_w)$ fed back from

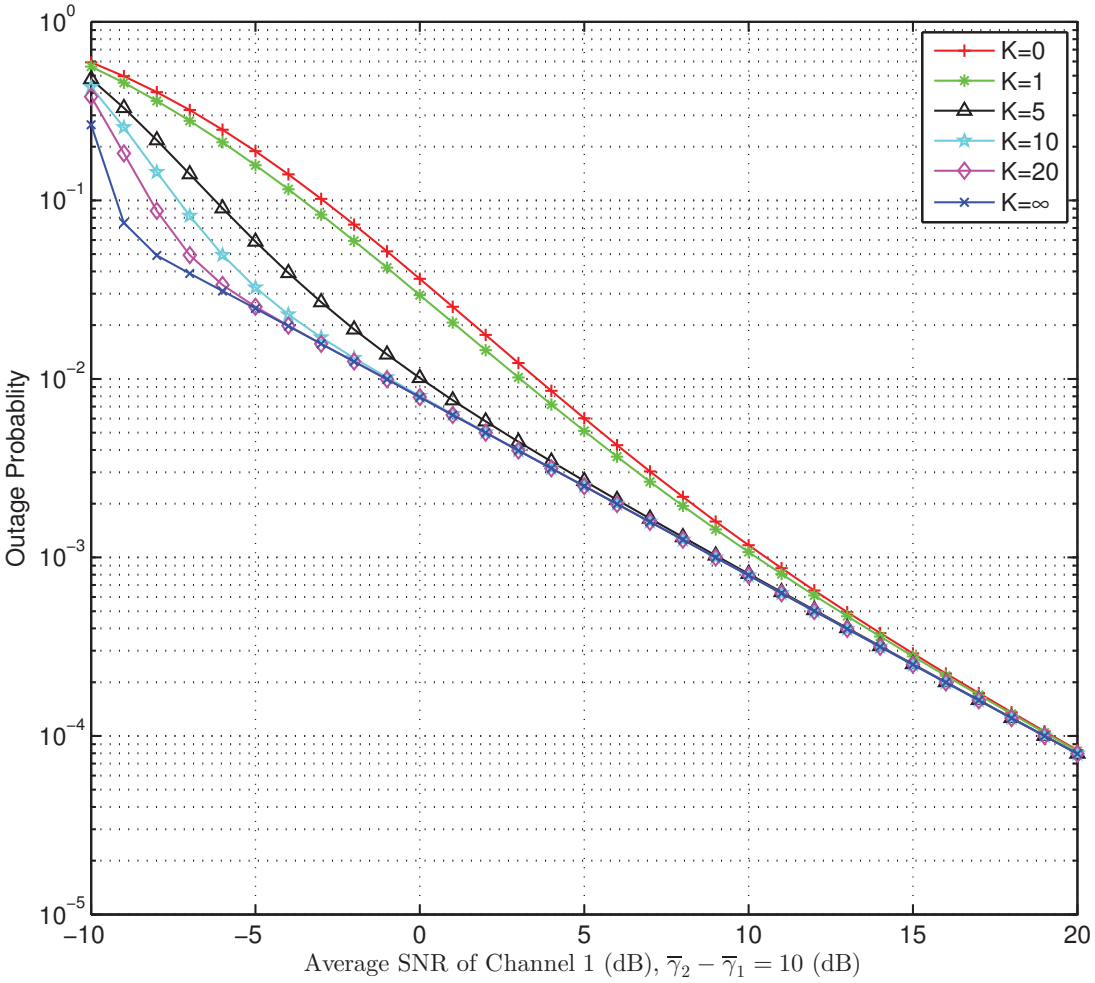

Figure 3.5: Outage probability with different K for $\overline{\gamma}_1 \neq \overline{\gamma}_2$.

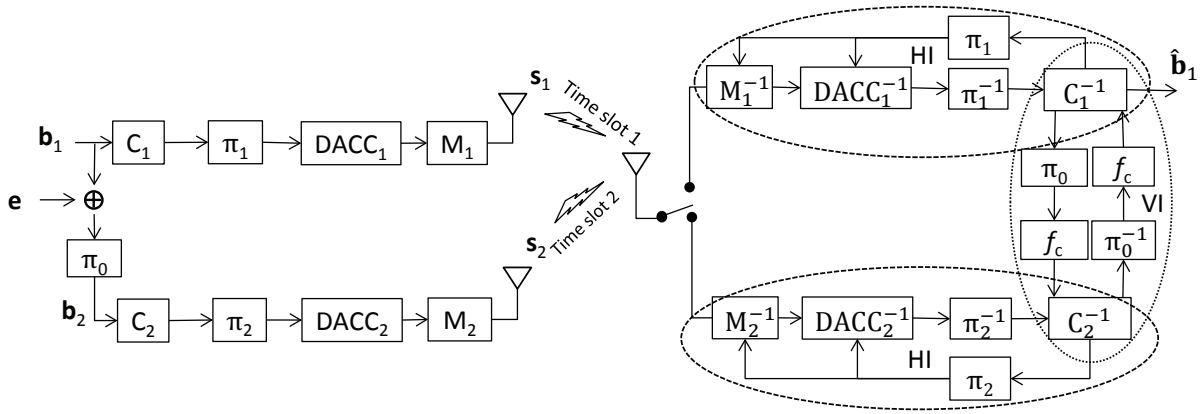

Figure 3.6: The schematic diagram of the Slepian-Wolf correlated sources transmission system.

the decoder corresponding to the *w-th* position of the labelling patterns, the demapper calculates the extrinsic LLR $L_e(b_v)$ of bit b_v in (3.25) [20] from the received signal y by

$$\begin{aligned} L_e(b_v) &= \ln \frac{P(b_v = 1|y))}{P(b_v = 0|y))} \\ &= \ln \frac{\sum_{s \in \mathbf{S}_1} \left\{ \exp\left(-\frac{\left|y - \sqrt{G}hs\right|^2}{2\sigma^2} \right) \prod_{w \neq v}^{M} \exp[b_w L_a(b_w)] \right\}}{\sum_{s \in \mathbf{S}_0} \left\{ \exp\left(-\frac{\left|y - \sqrt{G}hs\right|^2}{2\sigma^2} \right) \prod_{w \neq v}^{M} \exp[b_w L_a(b_w)] \right\}} \end{aligned} \tag{3.25}$$

where $\mathbf{S}_1$ and $\mathbf{S}_0$ indicate the sets of symbol sequence having v-th bit being 1 or 0. M is the number of bits per symbol (since we are assuming QPSK, M=2). The output extrinsic LLRs of demapper are processed by the de-accumulator $DACC_i^{-1}$ of $DACC_i$ and de-interleaved by the corresponding de-interleaver π_i^{-1}, then refined by decoders D_i^{-1} of the channel coder D_i using the BCJR algorithm [21], where $i = 1, 2$. The soft-decision output of D_i^{-1} is further fed back to $DACC_i^{-1}$ and demapper M_i^{-1} as a priori LLR [22]. This processes is independently performed for $\mathbf{s}_1$ and $\mathbf{s}_2$, and hence is referred to as Horizontal Iteration (HI).

Furthermore, during each HI loop, channel decoders C_1^{-1} and C_2^{-1} also exchange LLR with each other. The LLR updating function f_c [23] is used in this process to utilize the knowledge of source correlation (*bit-flipping* probability p_f between two sources) as,

$$f_c(x) = \ln \frac{(1 - p_f) \cdot \exp(x) + p_f}{(1 - p_f) + \exp(x) \cdot p_f} \tag{3.26}$$

where x is the extrinsic LLR of the information bits, output from C_1^{-1} and C_2^{-1}, respectively. This processes is referred to Vertical Iteration (VI). After sufficient VI iterations, we activate again the HI loop, and this process is repeated until no more significant gain of mutual information improvement can be achieved.

B. Simulation Results

In this sub-section, we demonstrate the comparison results between the theoretical outage and FER curves obtained through simulation. The setting of simulation parameters are given in Table. 3.1.

Fig. 3.7 shows the FER performance of the BICM-ID based Slepian-Wolf correlated sources transmission system we presented in the previous sub-section, where the theoretical outage curves are also plotted for comparison. It is found that the FER and theoretical outage curves exhibit the same decay; No diversity gain can be achieved when the two sources are independent ($p_f = 0.5$). If two information sequences are fully correlated ($p_f = 0$), the FER curve also can achieve sharper decay than $2nd$ order diversity. The results verify the asymptotic tendency analysis provided in the sub-sections 3.3.1 and 3.3.3. However, there is a 2$\sim$3 dB gap in average SNR between them. It is attributed to that the BICM-ID technique used in this system does not achieve close-capacity performance. By applying close-capacity achieving techniques, e.g.,[24, 25], the gap can further be reduced.

Fig. 3.8 show FER performance with the of Rician factor K as a parameter, for the bit-flipping probability $p_f = 0.001$. It is found that, since two sources are highly correlated, at the relatively low average SNR region, the FER curves can achieves near the $2nd$ order diversity when $K = 0$, and sharper decay than that with $2nd$ order diversity when $K > 0$. However, the decay of the outage curves always asymptotically converge into the $1st$ order diversity when average SNR increases. This observation is consistent to the tendency of the outage performance in Fig. 3.4, as well as asymptotic tendency analysis provided in sub-section 3.3.2.

3.5 Optimal Power Allocations

Since the resources allocated to wireless devices are limited, especially in terms of transmit power, optimal power allocation is of significant importance like designing communication systems. In this section, we investigate the optimal power allocation based on the Slepian-Wolf correlated sources transmission system. The object of this work is to minimizing the

Item	Setting
p_f	$\Pr(\mathbf{u}=0)=\Pr(\mathbf{u}=1)=1/2$
C_1,C_2	Rate 1/2, $[3,2]_8$, memory-1 non-recursive systematic convolutional code
ACC_1,ACC_2	Rate 1/2, $[3,2]_8$, memory-1 recursive systematic convolutional code
Doping Rate d	2
Frame Length N	10^5 bits
Frame	4000
Modulation	4PSK non-Gray mapping
Decoding Algorithm	BCJR
Horizontal Iteration Times	20
Vertical Iteration Times	5
Interleaver Length	10^5 bits

Table 3.1: The settings of simulation parameters.

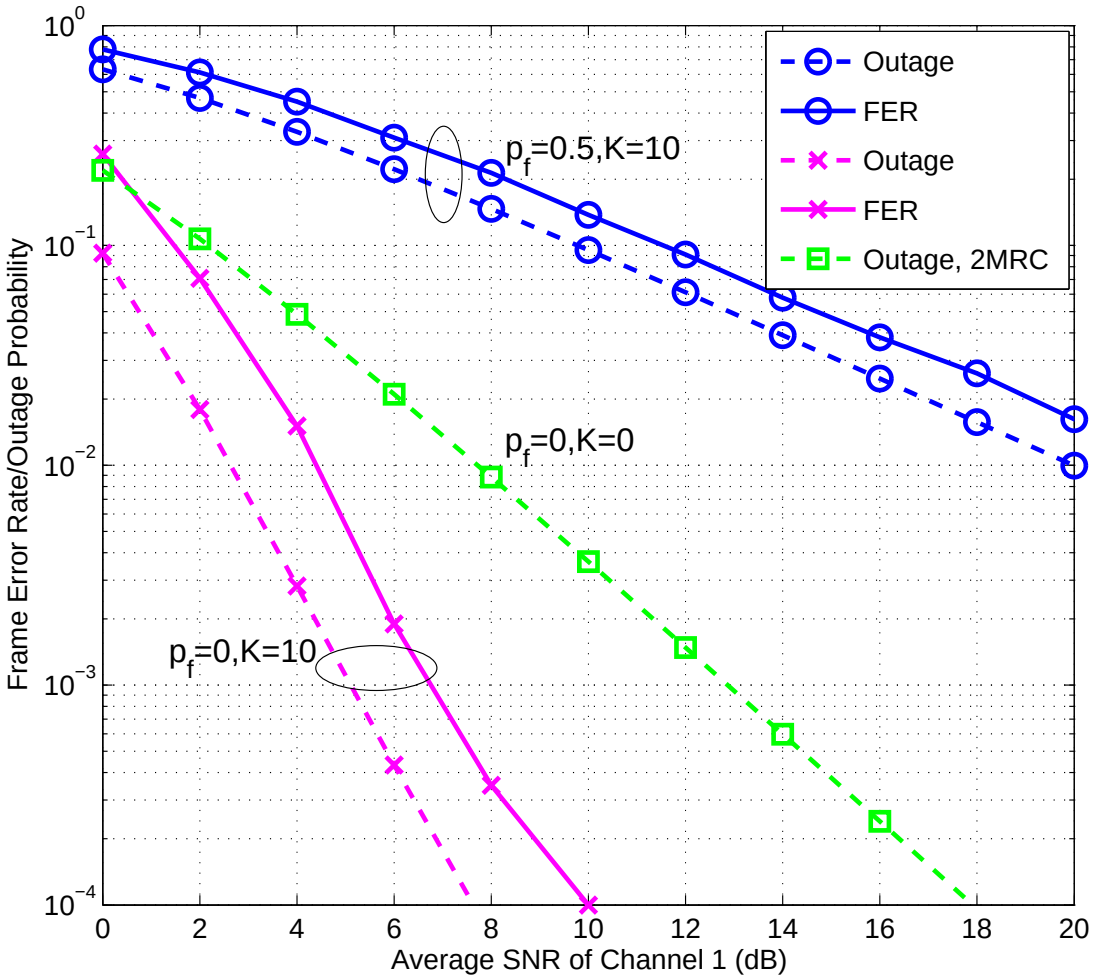

Figure 3.7: Comparison of the theoretical outage probability and the FER

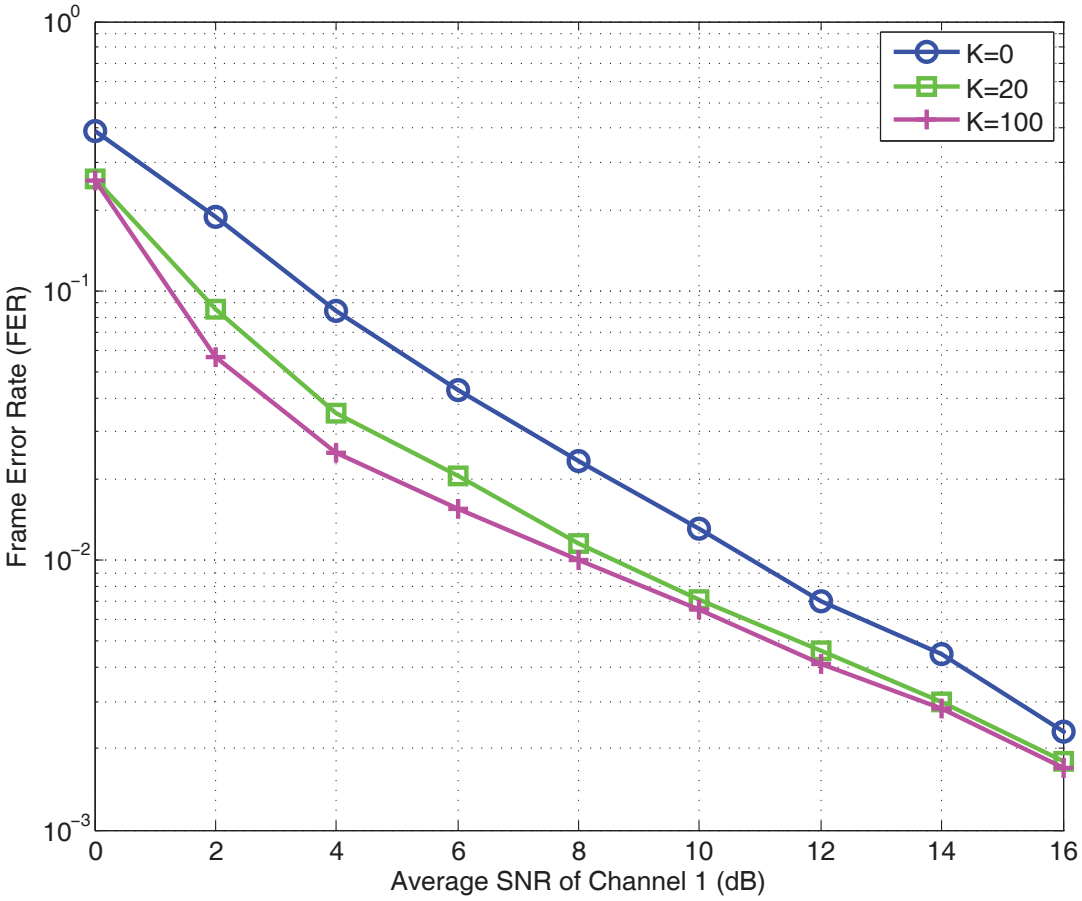

Figure 3.8: FER results of BICM-ID based Slepian-Wolf correlated sources transmission system with p_f=0.001

outage probability by adjusting the power allocated to the sources, where the condition that the total transmit power is kept constant.

3.5.1 Problem Definition

In this section, the total transmit power of the system is assumed to be fixed, and the noises variance ${\sigma_n}^2$ of the both channel is normalized to the unity, as

$$\begin{cases} E_1 + E_2 = E_T \\ E_1/E_T = \alpha \\ E_2/E_T = 1 - \alpha \\ {\sigma_n}^2 = 1, \end{cases} \tag{3.27}$$

where the E_1 and E_2 are the average transmit powers over the two channels, respectively, and E_T represents the transmit power totalling over Channel 1 and Channel 2. α indicates the ratio of the transmit power allocated to S_1 which is transmitted via Channel 1 (1-α the ratio to Channel 2). The goal of this section is to find the optimal α that minimizes the outage probability with the transmit SNR $E_T/{\sigma_n}^2$ and the Rician factor K as parameters.

Based on the assumption described in 3.27, the outage probability expressions corresponding to 3.13 and 3.14, are given by

$$P_1 = 1 - \exp\left(-\frac{2^{R_{c1}H(\mathbf{b}_1|\mathbf{b}_2)} - 1}{\alpha E_T}\right) \tag{3.28}$$

and

$$P_2 = \int_{\gamma_1=2^{R_{c1}H(\mathbf{b}_1|\mathbf{b}_2)}-1}^{2^{R_{c1}H(\mathbf{b}_1)}-1} \frac{1}{\alpha E_T} \cdot \exp\left(-\frac{\gamma_1}{\alpha E_T}\right) \left[1 - Q_1\left(\sqrt{2K}, \sqrt{2\left(1+K\right)\frac{2^{\left[R_{c2}H(\mathbf{b}_1,\mathbf{b}_2) - \frac{R_{c2}}{R_{c1}}\log_2(1+\gamma_1)\right]} - 1}{\left(1-\alpha\right)E_T}}\right)\right] d\gamma_1. \tag{3.29}$$

Using these expressions, we identify the α value that minimize the outage in the next sub-section.

3.5.2 Optimal Power Allocation Analysis

Fig. 3.9 illustrates the outage probability versus α with different Rician factor K values as a parameter for $p_f = 0$ and ${E_T}/{\sigma_n}^2 = 10$ dB. The x-axis represents the ratio α of transmit power allocated to S_1. The 100% point indicates that the transmit power totally allocated to S_1, and 50% point represents the transmit power allocated to both sources equally. It is found from Fig. 3.9 that if $\mathbf{b}_1$ and $\mathbf{b}_2$ are fully correlated, the lowest outage probability can be achieved when transmit power is equally allocated to the both sources, when $K = 0$. Obviously, the larger the K value is, the smaller outage probability can be achieved. It can also be found that, the optimal power ratio α that achieves the minimum outage probability becomes small as the K factor becomes larger. This is reasonable because when the fading variation with Channel 2 is reduced, we should allocate more power to S_2 which is transmitted via stable Rician Channel 2 than S_1 via Channel 1 suffering from Rayleigh fading.

Fig. 3.10 shows the power allocation ratio α versus the outage probability with the K factor as a parameter for $p_f = 0.01$ and ${E_T}/{\sigma_n}^2 = 10$ dB. Similarly, the larger the K value, the smaller the outage probability. However, in this case the optimal α value, which can achieves the smallest outage probability, changes toward to the opposite direction; when the K value increases, the optimal α value also increases. This indicates that although the larger the ratio of LOS component in Channel 2, the smaller the outage probability. However, the optimal allocation ratio differs, depending on the K factor value. This is because when $\mathbf{b}_1$ and $\mathbf{b}_2$ are not fully correlated, $\mathbf{b}_2$ is transmitted successfully over Channel 2 having strong LOS component, and hence and the errors, occuring in $\mathbf{b}_2$ can not be eliminated as the LOS component increase. This leads to a conclusion that allocating more power to S_2 which is transmitted via Channel 2 having strong LOS component can not help improve the outage performance. On the contrary, it is more effective to allocate more power to S_1 than to S_2 in such scenario.

3.6 Summary

In this chapter, we have derived the information theoretic bound for the outage probability of a Slepian-Wolf correlated sources transmission system. This system have two correlated binary sources transmitted over block fading channels, one suffering from block Rayleigh fading, and the other from block Rician fading. The source correlation is assumed to be represented by a *bit-flipping* model. Also, We have analyzed the asymptotic properties of

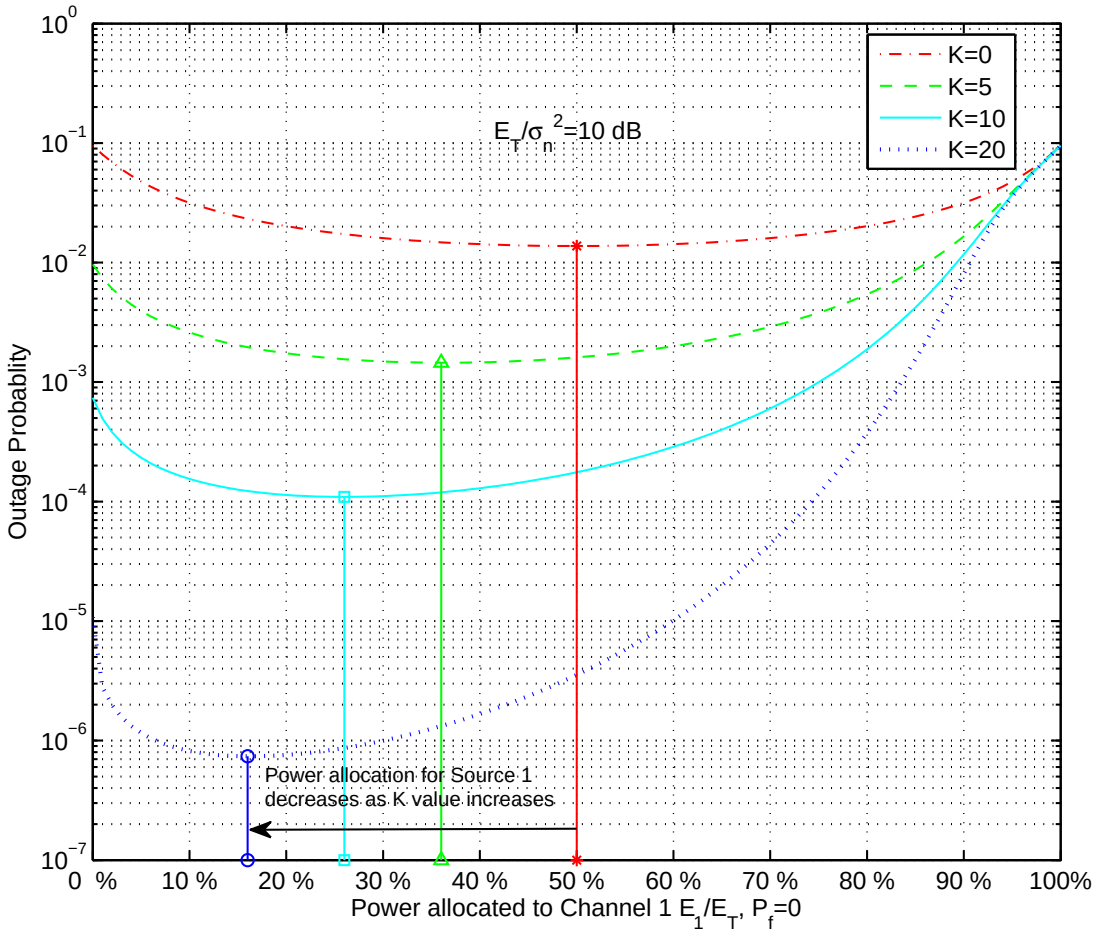

Figure 3.9: Optimal power allocation with different K for $p_f = 0$.

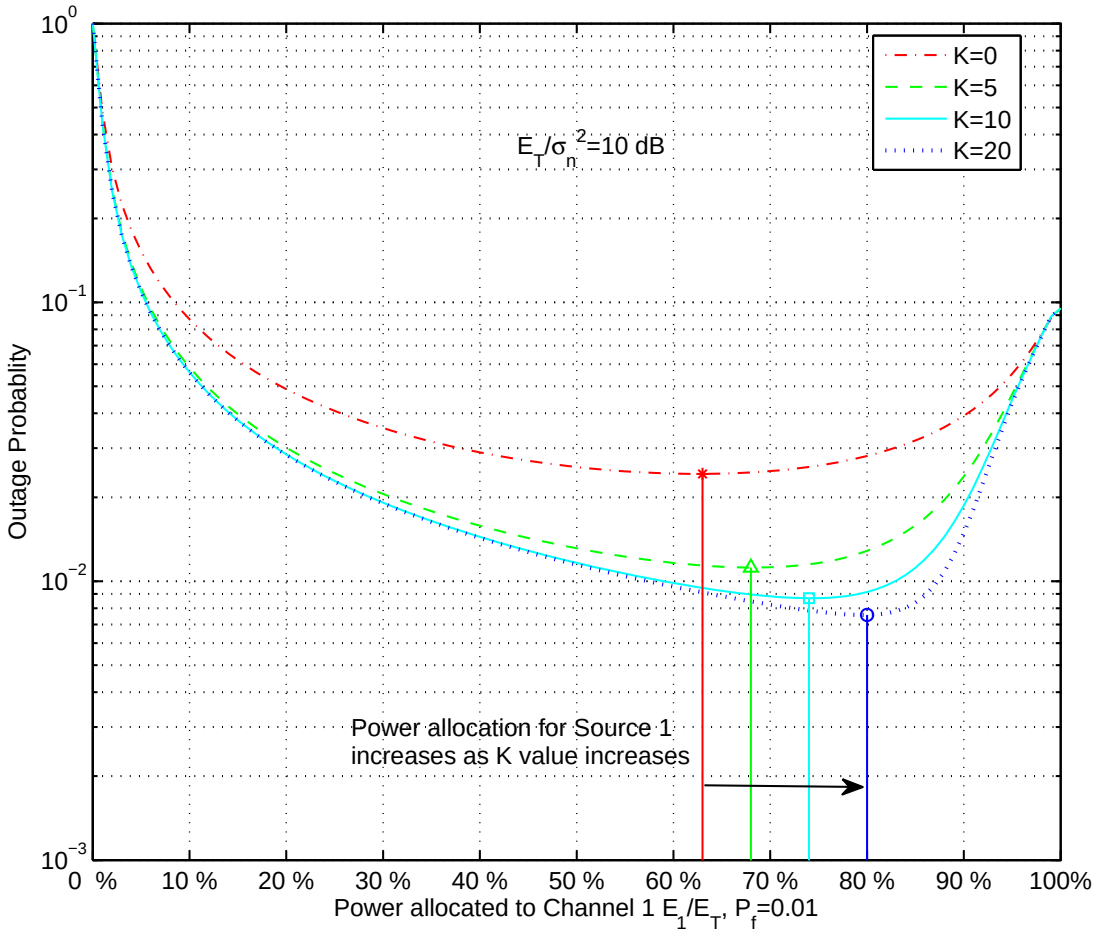

Figure 3.10: Optimal power allocation with different K for $p_f = 0.01$.

the outage performances. It has been found that when the two sources are fully correlated ($p_f = 0$), the outage curve can achieve sharper decay than the $2nd$ order diversity, as the LOS component power of the Rician fading channel increases. In the case $0 < p_f < 0.5$, the outage probability curves asymptotically plateau to the $1st$ order diversity. The turning point at which the outage starts to converge to such asymptotic tendency, depends on difference between the average SNR values $\overline{\gamma}_1$ and $\overline{\gamma}_2$.

This chapter also verified the consistency between the theoretical outage and FER curves. For verification purpose, we have conducted FER simulation assuming a BICM-ID based Slepian-Wolf correlated sources transmission system with LLR updating function f_c to utilize the correlation between the two sources. The comparison results show that the FER and the theoretical outage curves exhibit the same tendency.

Furthermore, the optimal power allocation is analytical identified under the condition that the total transmit power is fixed. The analytical results show that lower outage probability can not always be achieved by increasing the power ratio that allocated to source which is transmitted via Rician fading channels, so far as $p_f \neq 0$.

Chapter 4

Correlated Sources Transmission over Nakagami-m Fading Channels

In this chapter, we extend the works shown in **chapter 3** to more generic and practical case, which is the problem of two correlated sources transmitted to common destination over block Rayleigh and Nakagami-m fading channels.

First of all, the system model assumed in this chapter is introduced. The outage probability of this system is then derived based on the same technique used in the previous chapter. Furthermore, in several extreme cases, the closed-form expressions of the outage probability are derived theoretically. The asymptotic decay of the outage curves is derived based on the closed-form expression. Finally, the accuracy of theoretical results is also verified through computer simulations.

4.1 System and Channel Model

The system model used in this chapter is the same as that shown in Fig. 3.1 in the previous chapter. However, the distribution of the channel variation assumed in this chapter is based on the Nakagami-m channel model, which well suits the real channel behavior than Rician fading channel model. This is because the Nakagami-m distribution is derived from the measurement data gathered in real fields. In this chapter, Channel 1 connecting Source 1 (S_1) to Destination (D) suffers from Rayleigh fading, and Channel 2 connecting Source 2 (S_2) to D from Nakagami-m fading, as shown in Fig. 4.1. The PDF

of the instantaneous SNR γ suffering from the Nakagami-m fading is given by

$$p(\gamma) = \frac{m^m (\gamma)^{m-1}}{(\overline{\gamma})^m \Gamma(m)} \exp\left(-\frac{m\gamma}{\overline{\gamma}}\right), m > 0.5, \tag{4.1}$$

where $\Gamma(\cdot)$ is the complete Gamma function and $\overline{\gamma}$ represents the average SNR. The factor m represents the severity of fading variation. With m, the distribution is connected to the Rician distribution, by

$$m = \frac{(K+1)^2}{2K+1}, \tag{4.2}$$

with which (4.1) is approximately equivalent to the Rician distribution. With $m = \infty$, the channel is equivalent to a static AWGN channel, and with $m = 1$ the channel reduces to Rayleigh fading channel. In this chapter, we use (4.1) to represent the statistical characteristics of instantaneous SNRs in both Channel 1 and Channel 2. However, since the object of this work is to investigate the effect of information transmitted via Channel 2 which suffers from mild fading, throughout this chapter we assume $m = 1$ with Channel 1 indicating that Channel 1 is equivalent to Rayleigh fading. We also assume that the fading variation of Channel 2 statistically is independent of Channel 1. In this chapter, we study the impact of the factor m with Channel 2 and the *bit-flippin* probability p_f on the outage performance.

4.2 Outage Probability Derivation

In this section, the outage probability is derived theoretically. We employ the same technique as that used in **chapter 3** to define and to calculate the outage probability. According to the assumption that Channel 1 suffers from Rayleigh fading (m=1 with Nakagami-m distribution), P_1 denoting the probability that rate pair of R_{s1} and R_{s2} falls into the inadmissible area 1 in Fig. 3.2 can be expressed as,

$$\begin{aligned} P_1 &= \int_{\gamma_1=0}^{2^{R_{c1}H(\mathbf{b}_1|\mathbf{b}_2)}-1} p(\gamma_1)d\gamma_1 \int_{\gamma_2=0}^{\infty} p(\gamma_2)d\gamma_2 \\ &= \frac{\gamma\left(m, m\frac{2^{R_{c1}H(\mathbf{b}_1|\mathbf{b}_2)}-1}{\overline{\gamma}_1}\right)}{\Gamma(m)} \\ &\overset{\text{m=1}}{=} 1 - \exp\left(-\frac{2^{R_{c1}H(\mathbf{b}_1|\mathbf{b}_2)}-1}{\overline{\gamma}_1}\right). \end{aligned} \tag{4.3}$$

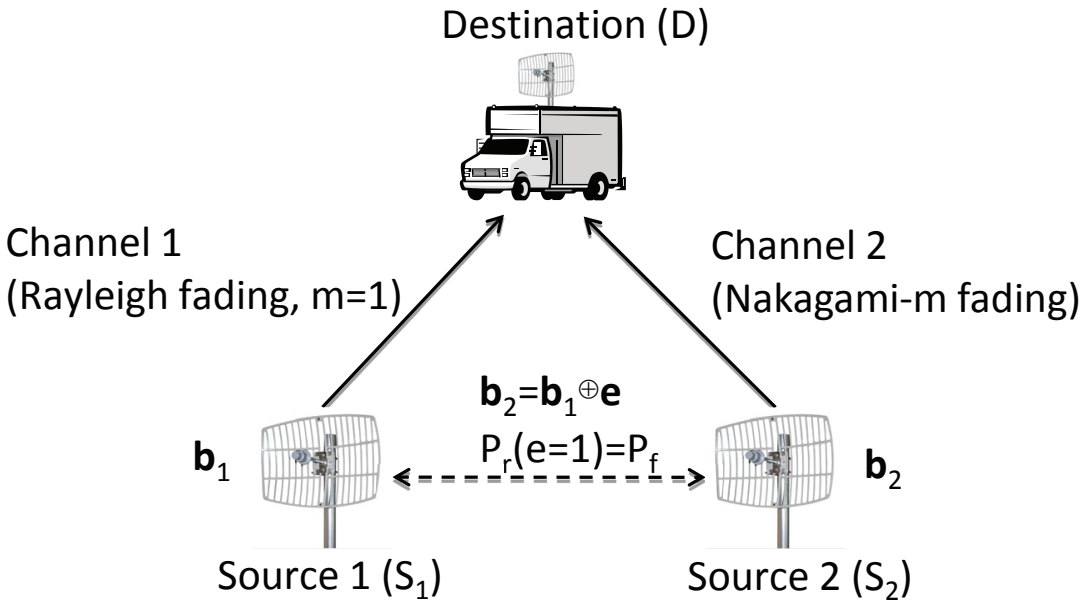

Figure 4.1: System model for Slepian-Wolf correlated sources transmission system: Nakagami-m fading channel scenario.

P_2 denoting the probability that rate pair R_{s1},R_{s2} falls into the inadmissible area 2 in Fig. 3.2 can be calculated as

$$\begin{aligned} P_2 &= \int_{\gamma_1=2^{R_{c1}H(\mathbf{b}_1|\mathbf{b}_2)}-1}^{2^{R_{c1}H(\mathbf{b}_1)}-1} p(\gamma_1) \int_{\gamma_2=0}^{2^{\left[R_{c2}H(\mathbf{b}_1,\mathbf{b}_2)-\frac{R_{c2}}{R_{c1}}\log_2(1+\gamma_1)\right]}-1} p(\gamma_2)d\gamma_2 d\gamma_1 \\ &= \int_{\gamma_1=2^{R_{c1}H(\mathbf{b}_1|\mathbf{b}_2)}-1}^{2^{R_{c1}H(\mathbf{b}_1)}-1} \frac{1}{\overline{\gamma}_1}\exp\left(-\frac{\gamma_1}{\overline{\gamma}_1}\right) \frac{\gamma\left(m, m\frac{2^{\left[R_{c2}H(\mathbf{b}_1,\mathbf{b}_2)-\frac{R_{c2}}{R_{c1}}\log_2(1+\gamma_1)\right]}-1}{\overline{\gamma}_1}\right)}{\Gamma(m)} d\gamma_1, \end{aligned} \tag{4.4}$$

where $\gamma(\cdot,\cdot)$ is the lower incomplete Gamma function [26]. It is found that only P_2 depends on the m value of Channel 2. According to [27, eq.(8.352.6)] P_2 can be expressed as

$$\begin{aligned} P_2 = &\int_{\gamma_1=2^{R_{c1}H(\mathbf{b}_1|\mathbf{b}_2)}-1}^{2^{R_{c1}H(\mathbf{b}_1)}-1} \frac{1}{\overline{\gamma}_1}\exp\left(-\frac{\gamma_1}{\overline{\gamma}_1}\right)\frac{(m-1)!}{\Gamma(m)} \\ &\cdot\left[1-\exp\left(-m\frac{2^{\left[R_{c2}H(\mathbf{b}_1,\mathbf{b}_2)-\frac{R_{c2}}{R_{c1}}\log_2(1+\gamma_1)\right]}-1}{\overline{\gamma}_1}\right)\sum_{k=0}^{m-1}\frac{\left(m\frac{2^{\left[R_{c2}H(\mathbf{b}_1,\mathbf{b}_2)-\frac{R_{c2}}{R_{c1}}\log_2(1+\gamma_1)\right]}-1}{\overline{\gamma}_1}\right)^k}{k!}\right] d\gamma_1. \end{aligned} \tag{4.5}$$

Furthermore, according to the Taylor expansion, we have

$$\exp(-x) = \sum_{n=0}^{\infty}\frac{(-x)^n}{n!} \approx 1-x,\ as\ x\to 0. \tag{4.6}$$

Then, (4.5) can be approximated as

$$\begin{aligned} P_2 \approx &\int_{\gamma_1=2^{R_{c1}H(\mathbf{b}_1|\mathbf{b}_2)}-1}^{2^{R_{c1}H(\mathbf{b}_1)}-1} \frac{1}{\overline{\gamma}_1}\left(1-\frac{\gamma_1}{\overline{\gamma}_1}\right)\frac{(m-1)!}{\Gamma(m)} \\ &\cdot\left[1-\left(1-m\frac{2^{\left[R_{c2}H(\mathbf{b}_1,\mathbf{b}_2)-\frac{R_{c2}}{R_{c1}}\log_2(1+\gamma_1)\right]}-1}{\overline{\gamma}_1}\right)\sum_{k=0}^{m-1}\frac{\left(m\frac{2^{\left[R_{c2}H(\mathbf{b}_1,\mathbf{b}_2)-\frac{R_{c2}}{R_{c1}}\log_2(1+\gamma_1)\right]}-1}{\overline{\gamma}_1}\right)^k}{k!}\right] d\gamma_1, \end{aligned} \tag{4.7}$$

which can easily be evaluated by some numerical method.

4.3 Closed-form Derivation

4.3.1 $m = 1$ with Channel 2

When $m = 1$ with Channel 2, the Nakagami-m distribution reduces to Rayleigh distribution. By assuming that the fading variation of the two channels are statistically independent and the spectrum efficiency of the transmission chain representing the coding rate and the multiplicity of the modulation for both channels are equal to one, i.e., R_{c1}=R_{c2}=1, (4.7) can be reduced to

$$\begin{aligned} P_2 =& \frac{1}{\overline{\gamma}_1} \int_{\gamma_1=2^{R_{c1}H(\mathbf{b}_1)}-1}^{2^{R_{c1}H(\mathbf{b}_1)}-1} \left[\left(1 - \frac{\gamma_1}{\overline{\gamma}_1}\right) - \left(1 - \frac{\gamma_1}{\overline{\gamma}_1} + \frac{1}{\overline{\gamma}_2} - \frac{2^{H(\mathbf{b}_1,\mathbf{b}_2)}}{\overline{\gamma}_2\,(1+\gamma_1)}\right)\right] d\gamma_1 \\ =& \frac{2^{H(\mathbf{b}_1,\mathbf{b}_2)} \ln\left(\frac{2^{H(\mathbf{b}_1)}}{2^{H(\mathbf{b}_1|\mathbf{b}_2)}}\right) - 2^{H(\mathbf{b}_1)} + 2^{H(\mathbf{b}_1|\mathbf{b}_2)}}{\overline{\gamma}_1\overline{\gamma}_2}. \end{aligned} \tag{4.8}$$

4.3.2 $m = 2$ with Channel 2

When $m = 2$ with Channel 2, it has mild fading compared to Channel 1. In this case, (4.7) can be explicitly express as

$$\begin{aligned} P_2 =& \int_{\gamma_1=2^{R_{c1}H(\mathbf{b}_1|\mathbf{b}_2)}-1}^{2^{R_{c1}H(\mathbf{b}_1)}-1} \left[\left(\frac{2\gamma_1 \left(\frac{2^{H(\mathbf{b}_1,\mathbf{b}_2)}}{1+\gamma_1} - 1\right)}{\overline{\gamma}_1^2\overline{\gamma}_2} \right) + \left(\frac{4\left(\frac{2^{H(\mathbf{b}_1,\mathbf{b}_2)}}{1+\gamma_1} - 1\right)^2}{\overline{\gamma}_1\overline{\gamma}_2^2} \right) \right] d\gamma_1 \\ =& \frac{2^{H(\mathbf{b}_1,\mathbf{b}_2)+1}(2^{H(\mathbf{b}_1)} - 2^{H(\mathbf{b}_1|\mathbf{b}_2)} - \ln\frac{2^{H(\mathbf{b}_1)}}{2^{H(\mathbf{b}_1|\mathbf{b}_2)}}) - (2^{H(\mathbf{b}_1)}-1)^2 - (2^{H(\mathbf{b}_1|\mathbf{b}_2)}-1)^2}{\overline{\gamma}_1^2\overline{\gamma}_2} \\ &+ \frac{-2^{2H(\mathbf{b}_1,\mathbf{b}_2)+2-H(\mathbf{b}_1)} + 2^{2H(\mathbf{b}_1,\mathbf{b}_2)+2-H(\mathbf{b}_1|\mathbf{b}_2)} - 2^{H(\mathbf{b}_1,\mathbf{b}_2)+3}\ln\frac{2^{H(\mathbf{b}_1)}}{2^{H(\mathbf{b}_1|\mathbf{b}_2)}} + 4(2^{H(\mathbf{b}_1)} + 2^{H(\mathbf{b}_1,\mathbf{b}_2)})}{\overline{\gamma}_1\overline{\gamma}_2^2}. \end{aligned} \tag{4.9}$$

(4.8) and (4.9) are used for asymptotic analysis in section 4.5.

4.4 Asymptotic Analysis

4.4.1 Asymptotic Tendency 1: Independent Sources Case

When $\mathbf{b}_1$ and $\mathbf{b}_2$ are independent ($p_f = 0.5$), $H(\mathbf{b}_1|\mathbf{b}_2) = H(\mathbf{b}_1)$. Hence, the probability P_2 is equal to 0, according to (4.4). Consequently, the outage probability is entirely

dominated by P_1, i.e., P_{out}=P_1. Moreover, since $\mathbf{b}_1$ and $\mathbf{b}_2$ are independent, $H(\mathbf{b}_1|\mathbf{b}_2) = 1$. Therefore, P_1 are the same as the outage probability in single Rayleigh fading channel, as

$$P_{\text{out,Rayleigh}} = 1 - \exp\left(-\frac{2^{R_{c1}} - 1}{\overline{\gamma}_1}\right) \approx \frac{2^{R_{c1}} - 1}{\overline{\gamma}_1}, \tag{4.10}$$

which corresponds to the $1st$ order diversity. It should be noticed that this conclusion is consistent to the analytical result of Rician channel's case, provided in sub-section 3.3.1.

4.4.2 Asymptotic Tendency 2: Large Average SNRs' Case

When average SNRs $\overline{\gamma}_1 \to \infty$ and $\overline{\gamma}_2 \to \infty$, the outage probability $P_2 \to 0$ because the incomplete Gamma Funcion in (4.4) approaches 0, as the second parameter of $\gamma(\cdot,\cdot)$ becomes small. Therefore, only P_1 dominates the outage probability in this case. Furthermore P_1 can also be expressed by the Taylor expansion, as

$$P_1 = \sum_{n=0}^{\infty} \frac{(-1)^{(n)}}{n+1!} \left(\frac{2^{R_{c1}H(\mathbf{b}_1|\mathbf{b}_2)} - 1}{\overline{\gamma}_1}\right)^{n+1}. \tag{4.11}$$

However, (4.11) is dominated by the first term when $\overline{\gamma}_1$ is large. Thus, (4.11) can be approximated as:

$$P_1 \approx \frac{2^{R_{c1}H(\mathbf{b}_1|\mathbf{b}_2)} - 1}{\overline{\gamma}_1}, \tag{4.12}$$

which follows the $1st$ order diversity. Also, this tendency is consistent to the result of Rician channel's case, provided in sub-section 3.3.2.

4.5 Asymptotic Tendency in Fully Correlated Sources Case

When $\mathbf{b}_1$ and $\mathbf{b}_2$ are fully correlated ($p_f = 0$), $H(\mathbf{b}_1|\mathbf{b}_2) = 0$ and $H(\mathbf{b}_1, \mathbf{b}_2) = 1$. Therefore, the probability P_1 is equals to 0, according to (4.3). Hence, the outage probability is completely dominated by P_2, i.e., P_{out}=P_2.

4.5.1 $m = 1$ with Channel 2

When $\mathbf{b}_1$ and $\mathbf{b}_2$ are fully correlated ($p_f = 0$), (4.8) is reduced to

$$P_2 = \frac{2\ln 2 - 1}{\overline{\gamma}_1 \overline{\gamma}_2}. \tag{4.13}$$

We can see P_{out} ($=P_2$) is inversely proportional to the product of $\overline{\gamma}_1$ and $\overline{\gamma}_2$, which follow the $2nd$ order diversity. This is because there are two independent branches connected to the common destination, when information bits transmitted via the two branches are entirely correlated, resulting in fully cooperative diversity [26] order achieved.

4.5.2 $m = 2$ with Channel 2

When $m = 2$ with Channel 2, (4.9) is reduced to

$$P_2 = \left(\frac{3 - 4\ln 2}{\overline{\gamma}_1^2 \overline{\gamma}_2}\right) + \left(\frac{12 - 16\ln 2}{\overline{\gamma}_1 \overline{\gamma}_2^2}\right). \tag{4.14}$$

It is obvious that P_{out} ($=P_2$) is inversely proportional to the $3rd$-order power of the average SNRs $\overline{\gamma}_1$ and $\overline{\gamma}_2$, hence the decay of the outage curve is sharper than the $2nd$ order diversity. It should be noticed that, in the system model we discuss in this chapter, the destination can receive information only from two independent branches. Therefore the full cooperative diversity order that can be achieved is, in theory, 2. However, since the outage probability of Nakagami-m fading channels has the relationship with the factor m [28] as,

$$P_{out,Nakagami-m} \propto (\overline{\gamma})^{-m}, \tag{4.15}$$

the decay is shaper than $2nd$ order diversity, in FER as well as the outage performance is also a function the value of m. The contribution of $3rd$-order power of average SNRs that appears in the denominator in (4.14) comes from relatively mild fading with Channel 2.

4.6 Numerical Results and Discussion

In this section, the numerical results of the theoretical outage probability are presented. Here, the lengths of Channel 1 and Channel 2 are assumed to be the same, and we ignore shadowing. Therefore, average SNRs $\overline{\gamma}_1 = \overline{\gamma}_2$. Fig. 4.2 shows the theoretical

outage probability versus average SNR with p_f as a parameter, for m=1 with Channel 2, indicating that the severity of fading variation in Channel 2 is the same as in Channel 1. It is found that, the $2nd$ order diversity can be achieve only if $p_f = 0$ over the entire range of the average SNR. The outage performances shown in Fig. 4.2 are consistent to the theoretical analysis result provided in sub-section 4.5.1.

In Fig. 4.3, the theoretical outage probability versus average SNRs $\overline{\gamma}_1 = \overline{\gamma}_2$ are presented with p_f as a parameter, for $m = 2$ with Channel 2, indicating that fading variation of Channel 2 is not as severe as that of Channel 1. We can see that no diversity gain can be achieved when $p_f = 0.5$. It should be noticed that, the lower the p_f value, the smaller the outage probability. The outage probability can achieve sharper decay than that with the $2nd$ order diversity if $\mathbf{b}_1$ and $\mathbf{b}_2$ are fully correlated ($p_f = 0$). However, if $p_f \neq 0$, the decay of the outage curve asymptotically converges into that of the $1st$ order diversity. The results are consistent to the theoretical analysis result provided in sub-section 4.4.1 and 4.5.2. One can easily observe from Fig. 4.2 and Fig. 4.3 that the theoretical curves obtained by a numerical integration technique are consistent to the asymptotic analysis results. As expected, the milder fading variation of Channel 2, the lower the outage probability. Compared with the case of $m = 1$, relatively lower outage probability can be achieved with $m = 2$ at the same average SNR value.

Fig. 4.4 demonstrates the outage probability curves with the factor m as a parameter, where the *bit-flipping* probability is fixed at $p_f = 0.01$, indicating that $\mathbf{b}_1$ and $\mathbf{b}_2$ are highly correlated, but $\mathbf{b}_2$ still contains some flipped bits. It is found, again interestingly, that when the average SNRs $\overline{\gamma}_1$ and $\overline{\gamma}_2$ are small, the outage probability reduces quickly, however, the decay of the outage curves always asymptotically converges into the $1st$ order diversity when the $\overline{\gamma}_1$ and $\overline{\gamma}_2$ increase, regardless of the severity of fading variation of Channel 2. This observation is also exactly consistent to the asymptotic tendency analysis result provided in sub-section 4.4.2. Although this asymptotic behaviour is the same as that shown in [3] and Fig. 3.4 in **chapter 3**, the convergence behaviour to the asymptotic performance is different and it, depends on different PDFs of Channel 2.

4.7 Consistency Verification between the Theoretical and Simulation Results for a Practical System

In this section, we present the results of the simulations conducted to evaluate the accuracy of theoretical analysis. The simulations were conducted based on the BICM-ID

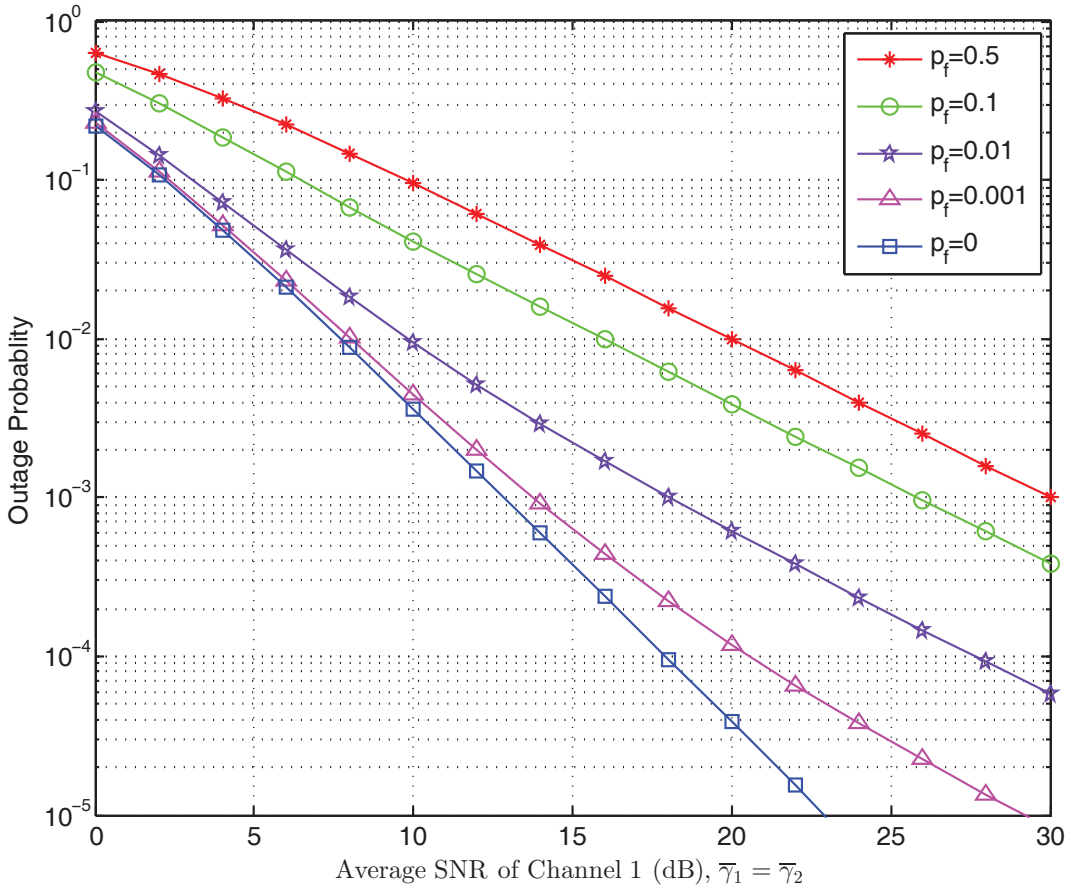

Figure 4.2: Outage probability with different p_f for $m = 1$.

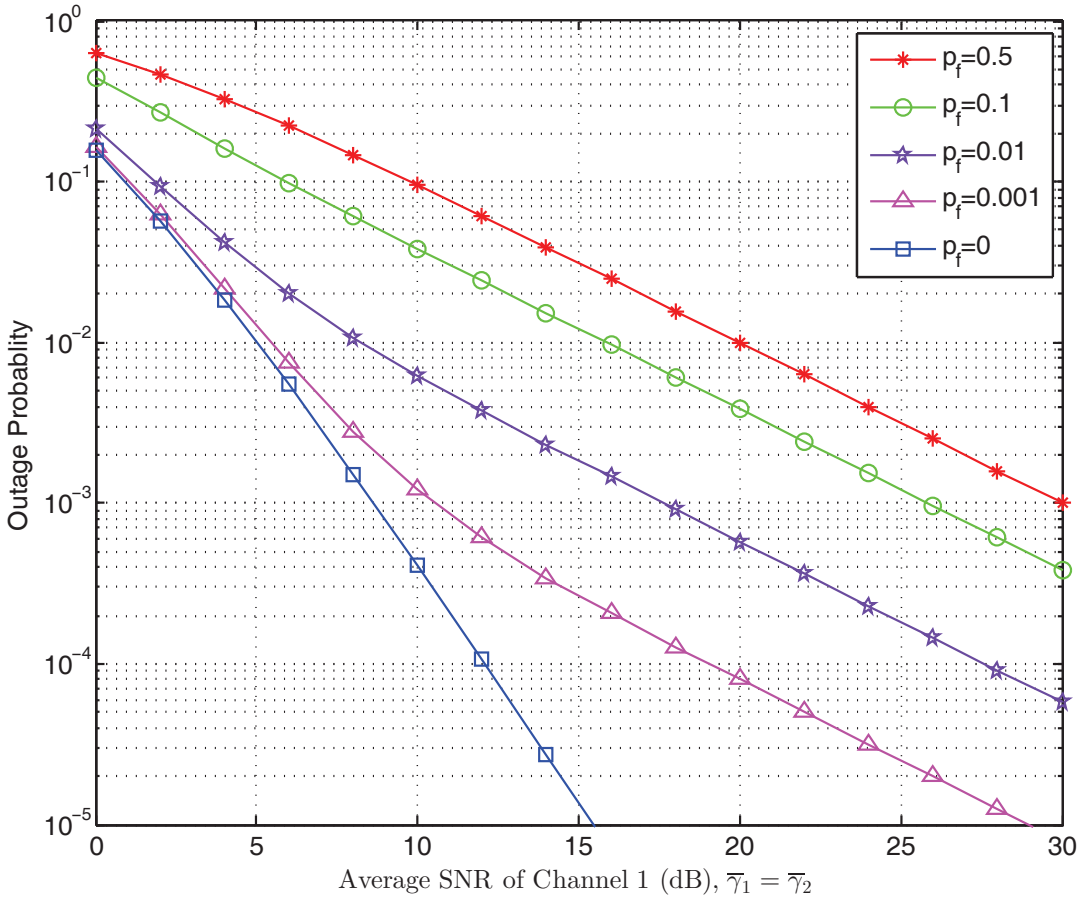

Figure 4.3: Outage probability with different p_f for $m = 2$.

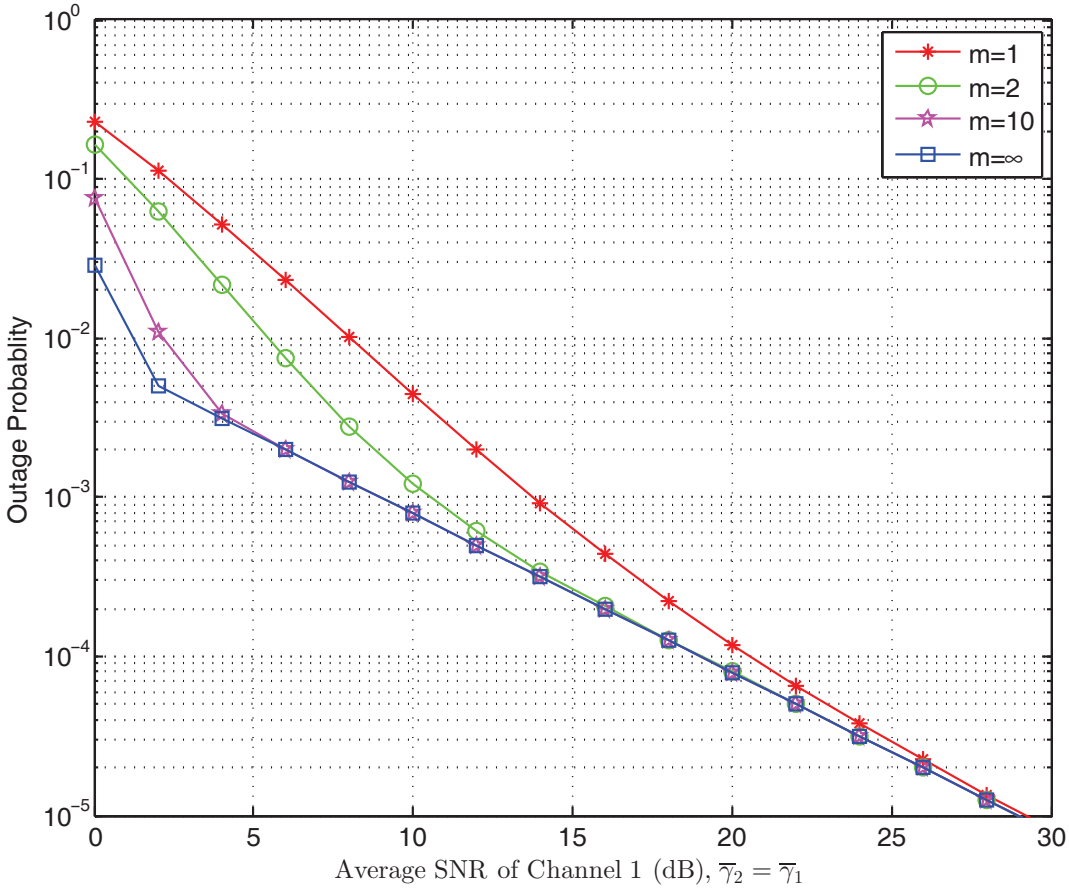

Figure 4.4: Outage probability with different m for $p_f = 0.01$.

based Slepian-Wolf correlated sources transmission system with same structure as Fig. 3.6 presented in the previous chapter. Unlike Fig. 3.6, the information bit sequence $\mathbf{b}_1$ and $\mathbf{b}_2$ are transmitted via Channels suffering from Nakagami-m fading, during the first and the second time slots, respectively. However, with $m = 1$, the Channel 1 reduces to Rayleigh distribution.

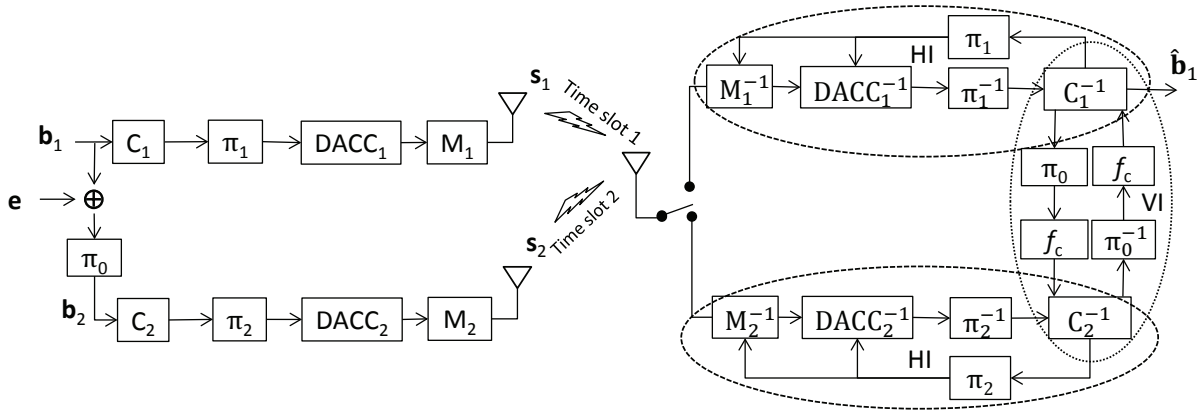

Figure 4.5: The schematic diagram of the Slepian-Wolf correlated sources transmission system.

The simulation results are present in Fig. 4.6, where the theoretical outage curves are also depicted for comparison. It can be observed from the figure that the FER performance curves show the same tendency as the outage analysis results. If the two sources are fully correlated, with m=1 for the both channels; the decay of the outage and FER curves exhibit the $2nd$ order diversity; the FER performance exhibits the same decay as outage curve, however, of which the decay is larger than the $2nd$ order diversity, when $m = 2$ with Channel 2.

4.8 Summary

In this chapter, we have derived the outage probability of a Slepian-Wolf correlated sources transmission system with two correlated binary sources over block Rayleigh and Nakagami-m fading channels. The source correlation is assumed to be represented by a *bit-flipping* model. A method for deriving the mathematical expressions of the outage probability is provided. The most significant contribution of this work is the derivation of closed-form expressions of the outage probabilities with several extreme cases. Based on the closed-form expression, asymptotic decay of the outage curves has been identified

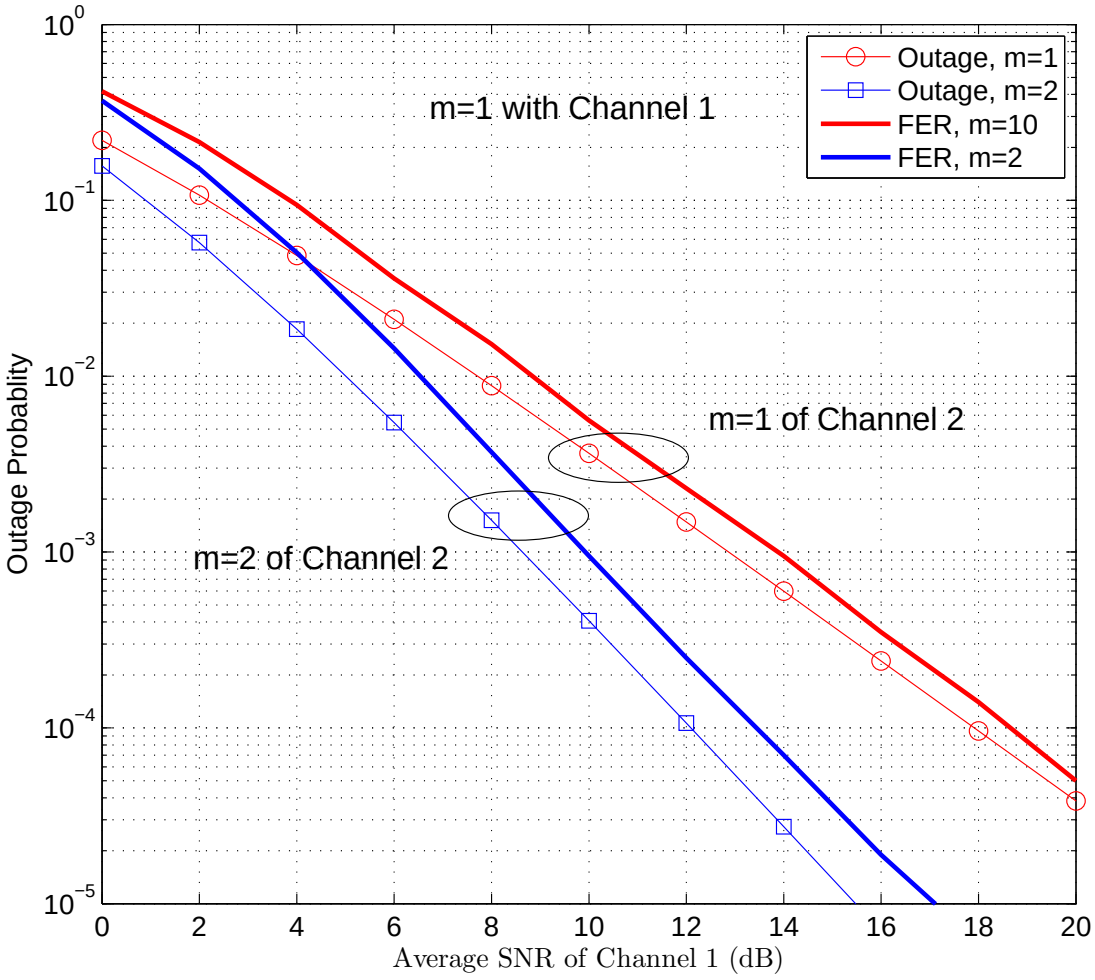

Figure 4.6: Comparison of the theoretical outage probability and the FER performance, p_f=0

theoretically. It has been shown that when the two sources are fully correlated ($p_f = 0$), 1) the decay of the outage curves is equal to the $2nd$ order diversity, when the both links are equivalent to Rayleigh channels (m=1 for Channel 1 and Channel 2); 2) when the fading variation of Channel 2 becomes mild (m=2), the outage curve exhibits sharper decay than that with the $2nd$ order diversity. It has also been shown that if $p_f \neq 0$, even with mild fading of Channel 2, the outage probability asymptotically plateaus to the $1st$ order diversity as the average SNRs of the both links become large. This indicates that asymptotically the contribution of the information bit sequence transmitted via Channel 2 diminishes as the average SNRs of the both links become large, so far as $p_f \neq 0$.

Chapter 5

Performance Dependency of the Channel Variation Statistics: Rician vs Nakagami-m Fading Channels

We evaluated the outage performance of correlated sources transmission over Rayleigh and Rician, as well as over Rayleigh and Nakagami-m fading channels in **chapter 3** and **chapter 4**, respectively. In this chapter, the impact of the distribution difference on the outage performance is analyzed theoretically.

The KullbackLeibler distance (KLD) between the Rician and Nakagami-m distributions is calculated as a function the factor K in Rician fading model and the factor m in Nakagami-m fading model, where as shown in (5.2). We then identify the different impact of Rician and Nakagami-m fading on outage performances of Slepian-Wolf correlated sources transmission system based on the KLD analysis results.

5.1 KLD between Rician and Nakagami-m Distributions

The Kullback-Leibler distance is a measure of the difference between two probability distributions. The definition of KLD for two continuous PDFs $p(x)$ and $q(x)$ is given as,

$$D_{KL}(p(x)||q(x)) = \int_X p(x) \ln \frac{p(x)}{q(x)} dx, \tag{5.1}$$

where X is the definition range of the random variable x. KLD is not a true distance between distributions since it is not symmetric. The KLD of $p(x)$ relative to $q(x)$ is generally not the same as the KLD of $q(x)$ relative to $p(x)$. The calculation results of KLD of the Rician relative to Nakagami-m distributions and the Nakagami-m relative to Rician distributions are summarized in Table.5.1, where $p(x)$ and $q(x)$ represent the Rician and Nakagami-m distributions, respectively. The function that determines the relationship between the factor K in Rician fading model and the factor m in Nakagami-m fading model is given as,

$$m = \frac{(K+1)^2}{2K+1}. \tag{5.2}$$

More in-depth observations, especially in terms of the relationship of the KLD to the outage performance is provided in the next section.

5.2 Outage Probability Comparison

Fig. 5.1 shows the KLD curves of the Rician relative to Nakagami-m distributions, as well as KLD of the Nakagami-m relative to Rician distributions, both as a function of the Rician factor K (correspondingly with m factor obtained from (5.2)). One can easily find from Fig. 5.1 that the KLD of Rician relative to Nakagami-m distributions $K_{LD}(p(x)||q(x))$ and the KLD of Nakagami-m relative to the Rician distributions $K_{LD}(q(x)||p(x))$ are not identical to each other, since the asymmetricity of KLD. However, both $K_{LD}(p(x)||q(x))$ and $K_{LD}(q(x)||p(x))$ exhibit a similar tendency, the KLDs between Rician and Nakagami-m distribution increases when the fading variation is relatively severe, when $K \leqslant 3$, and after that the KLDs gradually become smaller as K increases.

In Figs. 5.2 and 5.3, we compare the outage performances between the case Channel 2 is suffering from Rician and in another case Channel 2 from Nakagami-m, with the equivalent K and m given by (5.2). The analysis follows the results of **chapter 3** and **chapter 4**. Fig. 5.2 is for p_f=0 and Fig. 5.3 is for p_f=0.001. We can see from Figs. 5.2 and 5.3 that when both Rician and Nakagami-m fading reduce to Rayleigh fading ($K = 0$, $m = 1$, respectively), the outage performance is consistent with each other. When the values of K and m increase ($K = 3$, $m \approx 2.29$, respectively), the outage performance with Rician fading is well matched to the outage with Nakagami-m fading in the low average SNR region, but it can be clearly seen that there is a difference in the decay of the curves indicating the diversity order as the average SNR increases. However again the difference

K	m	$D_{KL}(p(x)\|\|q(x))$	$D_{KL}(q(x)\|\|p(x))$
0	0	0	0
1	1.33	0.0077	0.0063
2	1.8	0.0173	0.0115
3	2.29	0.0191	0.0113
4	2.77	0.0172	0.0098
5	3.27	0.0144	0.0083
6	3.77	0.0119	0.0071
8	4.76	0.0083	0.0055
10	5.76	0.0061	0.0044
12	6.76	0.0048	0.0037
14	7.76	0.0040	0.0031
16	8.76	0.0034	0.0027
18	9.76	0.0029	0.0024
20	10. 76	0.0026	0.0022

Table 5.1: The KLD between Rician and Nakagami-m distribution of different $K(m)$ values.

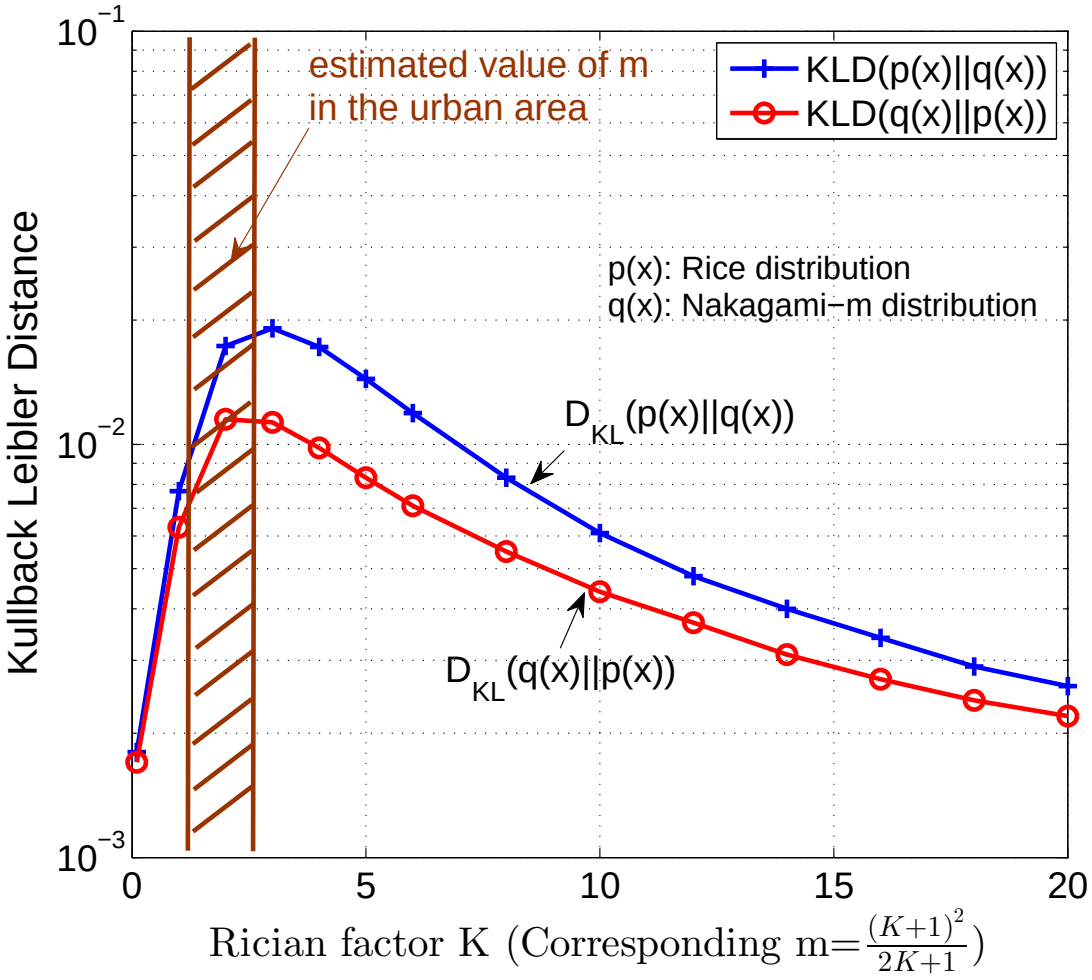

Figure 5.1: KLD between Rician and Nakagami-m distributions

becomes small when the K and m value becomes larger ($K = 20$,$m \approx 10.76$, respectively).

The m parameter in the urban area is in the range from 0.5 and 3.5 [29], as indicated by the shadow in Fig. 5.1. The relatively large KLD value between Rician and Nakagami-m distributions falls in this range. Hence the difference of achievable outage between Rician and Nakagami-m fading channels is correspondingly large. This result clearly indicate the theoretical limit for designing and/or evaluating the techniques for relaying system over Rayleigh and Rician fading channels, as well as over Rayleigh and Nakagami-m fading channels, respectively.

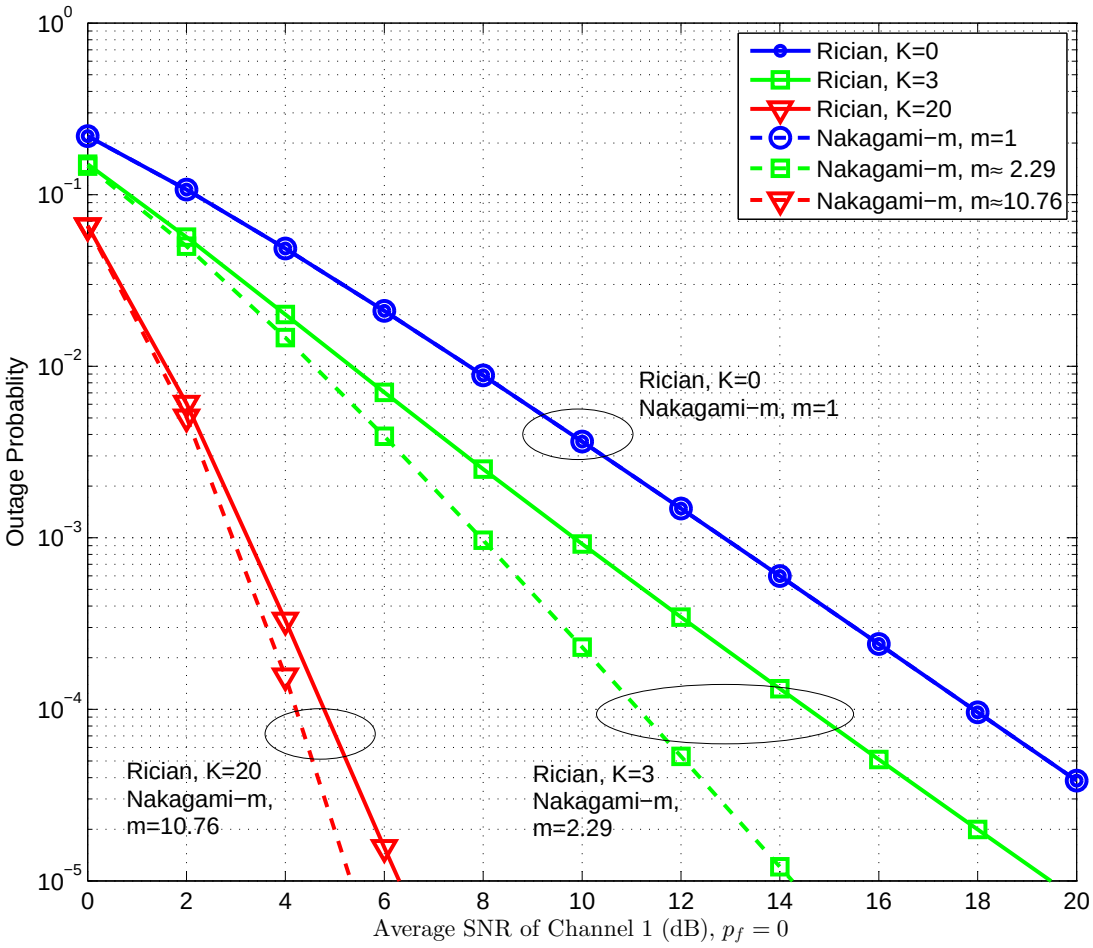

Figure 5.2: Outage probability comparison between Rician and Nakagami-m with different K (corresponding m).

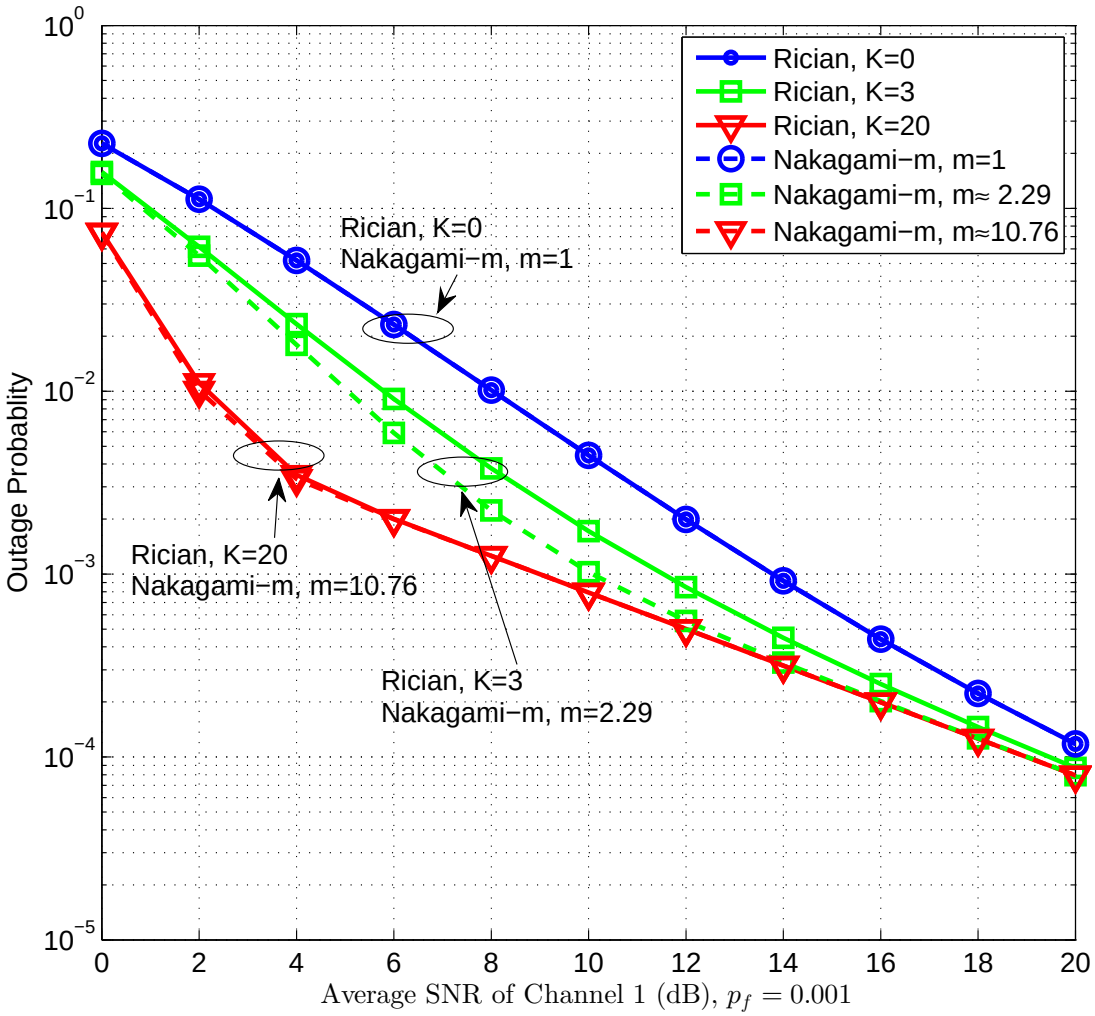

Figure 5.3: Outage probability comparison between Rician and Nakagami-m with different K (corresponding m).

Chapter 6

Conclusions and Future Work

6.1 Conclusions

In this thesis, we have investigated the two binary correlated sources transmission, where we analyzed the outage probability and identified the optimal power allocations of a Slepian-Wolf correlated sources transmission system. The novelty of this work is that we have assumed two correlated sources are transmitted over block fading channels where they have different statistical characteristics of the channel variations, one having LOS and NLOS components while the other only NLOS components. In this work, we derived the outage probability bound theoretically for the Slepian-Wolf correlated sources transmission system, and analyzed the asymptotic tendency of outage performance. To verify the consistency between the theoretical result and the reference result of exemplifying practical systems, a series of simulations have been conducted. This practical system assumed for the consistency verification is a BICM-ID system, where to improve the decoding performance, the LLR updating function exploiting the source correlation knowledge is utilized. Furthermore, we have addressed the KLD between Rician and Nakagami-m distributions and investigated the relationship between KLD and outage performance.

In **chapter 2**, we introduced the basic concept and background knowledge of this thesis, such as classfication of fading channels and their properties, receive diversity, and Slepian-Wolf theorem.

In **chapter 3**, two binary correlated sources transmitted through different fading channels are considered. In this work, one source information sequence is transmitted via Rayleigh fading channel composed of only NLOS components, while the other transmitted over Rician fading channel having both NLOS and LOS components. We first defined

the outage event and theoretically derived the outage probability expressions which can be evaluated by numerical techniques. The ***new*** result found by this work is that the outage curve exhibits sharper decay than that with $2nd$ order diversity if two sources are fully correlated. Another ***new*** outcome is that in the case the sources are not fully correlated, the outage curves exhibit very sharp decay at relatively low average SNR region, and then they asymptotically converge in to that with $1st$ order diversity as the average SNR increases. A series of simulations based on practical coding and decoding algorithm with BICM-ID were conducted to verify the consistency between simulation results and theoretical analysis results.

In **chapter 4**, we extend the system we used for outage probability analysis in **chapter 3** to cover more generic and realistic scenarios where the two binary correlated sources are transmitted via Rayleigh and Nakagami-m fading channels, respectively. Following the same definition and techniques as presented in **chapter 3**, we derived mathematical expression of the outage probability, and further obtained the closed-form expressions of the outage probability in several extreme cases. Based on the closed-form expressions, the asymptotic decay of the outage curves are derived theoretically. The results are consistent to that obtained in **chapter 3**. We found that if the two sources are fully correlated, the outage curves follow the $2nd$ order diversity when the factor m of the Nakagami-m fading is equal to one (namely Nakagami-m fading reduces to Rayleigh fading). This results is consistent to the results shown in [5] investigating two sources transmission over the Rayleigh fading channels. However, this thesis has theoretically revealed that the decay of the outage curve is sharper than the $2nd$ order diversity when the m factor value of Nakagami-m fading increases (namely fading variation become milder).

In **chapter 5**, we investigated the KLD between Rician and Nakagami-m distributions and evaluated impact of KLD on outage performances of the Slepian-Wolf correlated sources transmission system. It is well know that the Nakagami-m fading can approximate the Rician fading, however, in this work we found theoretically that when the variation of Rician and Nakagami-m fading become milder, the outage performance with Rician fading is well matched to the outage with Nakagami-m fading in the low average SNR region, but there is a difference in the decay of the curves in terms of the diversity order as the average SNR increases. However, again the difference of outage performance becomes small when the channel variation due to Rician and/or Nakagami-m fading further reduces.

6.2 Future Work

There are several issues that are planed to be challenged in the future, which are listed in the following:

1. In the problem of two correlated sources transmission, the code optimization was not considered in this thesis. More in-depth convergence property analysis by using Extrinsic Information Transfer (EXIT) chart [30, 31] for the BICM decoding process is need to optimize the coding chain. The EXIT-constrained Switching Algorithm (EBSA) [32] may identify the optimal mapping and coding parameters, which should be included in the future work.

2. In this thesis, we have derived closed-form outage probability expressions for Nakagami-m fading channels in the cases that factor $m = 1$ and $m = 2$. Closed-form expression derivation with arbitrary m value of Nakagami-m PDF should be provided in a closed-form outage expression relative to the Rician PDF, by utilizing the relationship between factor K and factor m, as,

$$m = \frac{(K+1)^2}{2K+1}. \tag{6.1}$$

3. In this thesis, only two correlated source transmission is considered. However, Slepian-Wolf theorem can be extend to arbitrary number of distributed source scenario [33, 34], as,

$$\sum_{j \in S} R_j \geqslant H(X(S)) \; for \; all \; S \subseteq [1:k]. \tag{6.2}$$

   We plan to work on multiple distributed sources scenarios, starting from three sources case, as shown in Fig. 6.2. In the case there are three correlated sources.

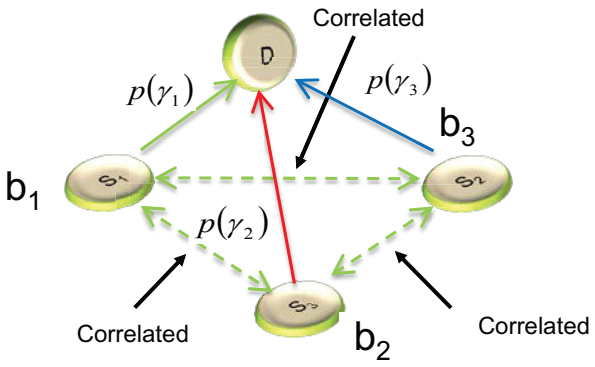

Figure 6.1: Triple correlated sources transmission.

The admissible rates region $\mathbb{R}_3$ in this case can be expressed as,

$$\begin{aligned} R_1 &\geqslant H(X_1|X_2, X_3), \\ R_2 &\geqslant H(X_2|X_1, X_3), \\ R_3 &\geqslant H(X_3|X_1, X_2), \\ R_1 + R_2 &\geqslant H(X_1, X_2|X_3), \\ R_1 + R_3 &\geqslant H(X_1, X_3|X_2), \\ R_2 + R_3 &\geqslant H(X_2, X_3|X_1), \\ R_1 + R_2 + R_3 &\geqslant H(X_1, X_2, X_3). \end{aligned} \tag{6.3}$$

Based on the definition of admissible rate region of the set $\mathbb{R}_3$ in (6.3), the outage probability can be calculate as,

$$P_{outage} = 1 - \int \cdots \int_{\mathbb{R}_3} p(\gamma_1)p(\gamma_2)p(\gamma_3)d\gamma_1 d\gamma_2 d\gamma_3 \tag{6.4}$$

4. In this thesis, the correlation parameter between the two sources is considered as a constant parameter in the theoretical analyses. As denoted before, the relaying is a straightforward application of correlated sources transmission. However, the source-relay link (intra-link) in relay system can not always be stable in practice, because the intra-link also suffers from fading. This indicates that the flipping probability p_f is time-varying. In this case, we can utilize the intra-link correlation by introducing the rate distortion function with the Hamming distortion measure, for the performance limit analysis. Then, we can calculate the outag probability in

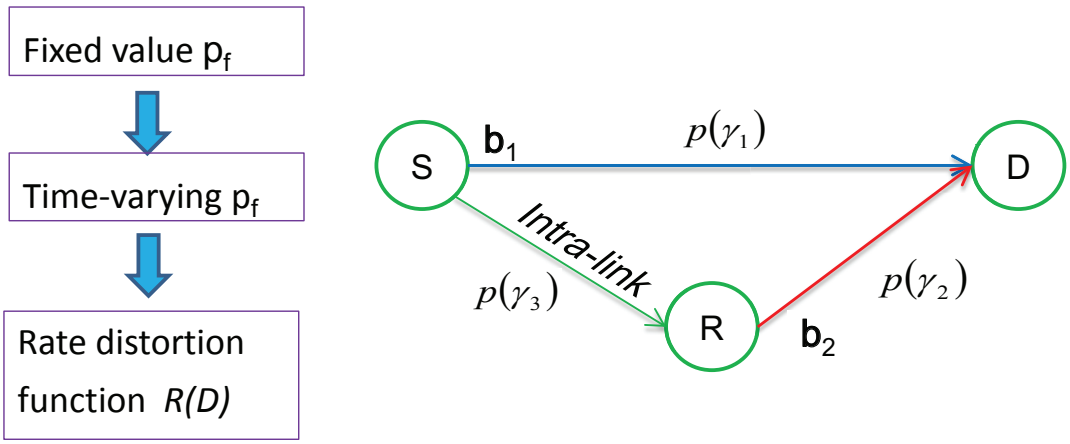

Figure 6.2: Intra-link correlation modelled by rate distortion function $R(D)$

this case, as,

$$P_{outage} = 1 - \int\limits_{\mathbb{R}_2, D} \int\int p(\gamma_1)p(\gamma_2)p(\gamma_3)d\gamma_1 d\gamma_2 d\gamma_3, \quad R(D) < \frac{1}{R_{c3}} \log(1+\gamma_3), \quad (6.5)$$

where $\mathbb{R}_2$, and D denote the admissible rate region specified by the Slepian-Wolf theorem and the rate distortion region specified by the lossy source-channel separation theorem, respectively. $R(D)$ is the binary rate distortion function, and R_{c3} is the spectrum efficiency of the transmission chain, including the channel coding scheme and modulation multiplicity within intra-link.

5. Resource allocation optimization including the following problems needs to be solved:

   - Give a proof for the existence global/local optima;
   - Minimize the outage probability while keeping the transmit power constant;
   - Minimize the transmit power while keeping the outage probability constant;
   - Diversity-Multiplexing-Trade-off (DMT) in the distributed coding system: identify the trade-off between diversity order and multiplexing order.

6. In this thesis, only the distributed lossless coding is considered. By allowing specified distortion level (lossy coding), we can further reduce the rates compared with the Slepian-Wolf region, as shown in Fig. 6.3. Consequently, the power and spectrum efficiencies can be further improved and robustness/flexibility can be enhanced.

This work is considered as paradigm shift from lossless to lossy based on distributed coding technique.

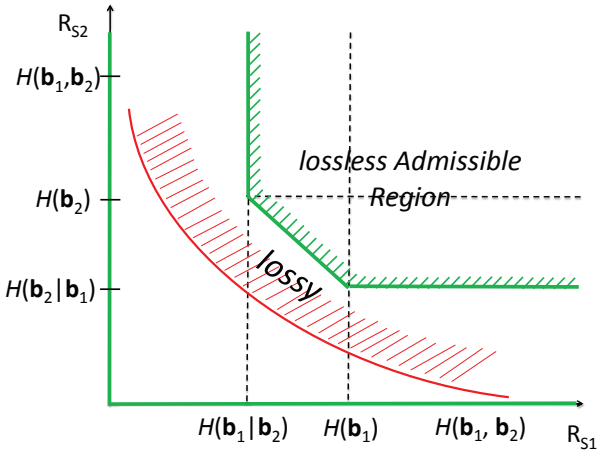

Figure 6.3: Lossy and Lossless region comparison.

This is a big challenge, because only for a specific case, Quadratic Gaussian Chief Executive Officer (CEO) problem [34], the bound of rate region, given distortion pair, is known. Even if the bound in generic cases can be derived, the outage calculation based on this bound is still expected to be difficult as well. Quality-of-service (QoS) also need to be considered when allocating the rate, power, and other resources in lossy multiple sources transmission.

Achievements

Conference Paper

- S. Qian, M. Cheng, K. Anwar, and T. Matsumoto, Outage probability analysis for correlated sources transmission over rician fading channels, presented in Personal Indoor and Mobile Radio Communications (PIMRC), 2013 IEEE 24rd International Symposium on 2013, in London. (peer-reviewed)

Oral Presentation

- S. Qian, M. Cheng, K. Anwar, and T. Matsumoto, Outage probability analysis for correlated sources transmission over Rician fading channels, presented in Steering Committee (STC) meeting of a JSPS-funded project, evaluated as excellent, in Osaka, March 2013.

Journal Papers

- S. Qian, M. Cheng, K. Anwar, and T. Matsumoto, Achievable outage probability for Slepian-Wolf relaying system over fading channels having different statistical properties, to be submitted to Electronics Letters.

Abbreviations and Notations

ACC	doped accumulator
ACC^{-1}	doped accumulator decoder
AF	amplify-and-forward
AWGN	additive white Gaussian noise
BCJR	MAP algorithm proposed by Bahl, Cocke, Jelinek, Raviv
BER	bit error rate
BICM-ID	bit-interleaved coded modulation with iterative detection
BPSK	binary phase-shift keying
CIS	channel state information
DACC	doped accumulator
$DACC^{-1}$	doped accumulator decoder
DF	decode-and-forward
EXIT	extrinsic information transfer
FER	frame error rate
HI	horizontal iteration
KLD	Kullback Leibler distance
LLR	log-likelihood ratio
LOS	line-of-sight
NLOS	non-line-of-sight
M	modulator
M^{-1}	demodulator
MAC	multiple access channel
MI	mutual information
MIMO	multiple-input-multiple-output
PDF	probability density function
CDF	cumulative density function
QPSK	quadrature phase-shift keying
SD	relay-destination
SR	source-relay
RD	relay-destination
VI	vertical iteration

$\oplus$	modulus 2 addition
$\hat{(\cdot)}$	estimation of the argument
$(\cdot)^{-1}$	inverse of the argument
$\exp(\cdot)$	exponential calculation of the argument
$E[\cdot]$	expectation of a random variable
$\ln(\cdot)$	natural logarithm to base e
$\log_2(\cdot)$	natural logarithm to base 2
$\log(\cdot)$	natural logarithm to any bases
$\max(\cdot)$	maximum value
$\min(\cdot)$	minimum value
$\text{sign}(\cdot)$	the sign of the argument
$H(\cdot)$	entropy
$H(\cdot\|\cdot)$	conditional entropy
$H(\cdot,\cdot)$	joint entropy

$\mathbf{b}_i$	information bit sequences at ith source
$\mathbf{s}_i$	modulated symbols from ith source
$\mathbf{e}_k$	the error sequence used at k-th sensor
C_i	i-th channel encoder
D	destination
ρ	correlation coefficient
D_i	decoder for encoder C_i
f_c	LLR updating function
$I(\cdot,\cdot)$	mutual information between argument 1 and 2
$I_0(\cdot)$	zero-*th* order modified Bessl's function of the first kind
I^{a}	*a priori* information
I^{e}	extrinsic information
K	Rician factor
L^{a}	*a priori* LLR sequence
L^{e}	extrinsic LLR sequence
L^{p}	*a posteriori* LLR sequence
m	shaper factor
p_f	bit flipping probability
$\Pr(\cdot)$	probability of the variable

$Q_1(\cdot,\cdot)$	Marcum Q-Function
$\Gamma(\cdot)$	complete Gamma function
$\gamma(\cdot,\cdot)$	lower incomplete Gamma function
R	relay
$R(D)$	rate distortion function
R_s	the source coding rate
R_c	spectrum efficiency considering both the channel coding rate and modulation multiplicity
S	source
Π	interleaver
Π^{-1}	de-interleaver
$\overline{\gamma}$	average SNR
γ	instantaneous SNR
σ^2	Gaussian noise variance

Bibliography

[1] A. Nosratinia, T. Hunter, and A. Hedayat, "Cooperative communication in wireless networks," *Communications Magazine, IEEE*, vol. 42, no. 10, pp. 74–80, 2004.

[2] Q. Li, R. Hu, Y. Qian, and G. Wu, "Cooperative communications for wireless networks: techniques and applications in lte-advanced systems," *Wireless Communications, IEEE*, vol. 19, no. 2, pp. –, 2012.

[3] M. Cheng, K. Anwar, and T. Matsumoto, "On the duality of source and channel correlations: Slepian-wolf relaying viewpoint," in *Communication Systems (ICCS), 2012 IEEE International Conference on*, pp. 388 –392, nov. 2012.

[4] M. Cheng, K. Anwar, and T. Matsumoto, "Outage analysis of correlated source transmission in block rayleigh fading channels," in *Vehicular Technology Conference (VTC Fall), 2012 IEEE*, pp. 1 –5, sept. 2012.

[5] M. Cheng, K. Anwar, and T. Matsumoto, "Outage probability of a relay strategy allowing intra-link errors utilizing slepian-wolf theorem," *EURASIP Journal on Advances in Signal Processing*, vol. 2013, no. 1, p. 34, 2013.

[6] K. Anwar and T. Matsumoto, "Accumulator-assisted distributed turbo codes for relay system exploiting source-relay correlations," *IEEE Communications Letters*, vol. 16, no. 7, pp. 1114–1117, 2012.

[7] D. Slepian and J. Wolf, "Noiseless coding of correlated information sources," *IEEE Transactions on Information Theory*, vol. 19, pp. 471– 480, July 1973.

[8] K. Anwar and T. Matsumoto, "Spatially concatenated codes with turbo equalization for correlated sources," *IEEE Transactions on Signal Processing*, vol. 60, pp. 5572–5577, October 2012.

[9] A. Goldsmith, *Wireless Communications*. Stanford University, USA: Cambridge University Press, 2005.

[10] X. Li and J. Ritcey, "Bit-interleaved coded modulation with iterative decoding," *Communications Letters, IEEE*, vol. 1, no. 6, pp. 169–171, 1997.

[11] X. Li and J. Ritcey, "Trellis-coded modulation with bit interleaving and iterative decoding," *Selected Areas in Communications, IEEE Journal on*, vol. 17, no. 4, pp. 715–724, 1999.

[12] H. Suzuki, "A statistical model for urban radio propogation," *Communications, IEEE Transactions on*, vol. 25, no. 7, pp. 673–680, 1977.

[13] U. Dersch and W. Braun, "A physical mobile radio channel model," in *Vehicular Technology Conference, 1991. Gateway to the Future Technology in Motion., 41st IEEE*, pp. 289–294, 1991.

[14] C. E. Shannon, "A mathematical theory of communication," *Bell Systems Technical Journal*, vol. 27, pp. 379–423,623–656, 1948.

[15] J. Garcia-Frias and Y. Zhao, "Near-shannon/slepian-wolf performance for unknown correlated sources over AWGN channels," *IEEE Transactions on Communications*, vol. 53, pp. 555–559, April 2005.

[16] S. Ray, M. Medard, M. Effros, and R. Koetter, "On separation for multiple access channels," in *Information Theory Workshop, 2006. ITW '06 Punta del Este. IEEE*, pp. 399–403, 2006.

[17] W. Gander and W. Gautschi, "Adaptive quadrature-revisited," *BIT*, vol. 40, pp. 84–101, 2000.

[18] A. Stefanov and E. Erkip, "Cooperative coding for wireless networks," *Communications, IEEE Transactions on*, vol. 52, no. 9, pp. 1470–1476, 2004.

[19] K. Anwar and T. Matsumoto, "Very simple bicm-id using repetition code and extended mapping with doped accumulator," *Wireless Personal Communications*, pp. 1–12, September 2011.

[20] S. Ten Brink, J. Speidel, and R.-H. Yan, "Iterative demapping and decoding for multilevel modulation," in *Global Telecommunications Conference, 1998. GLOBECOM 1998. The Bridge to Global Integration. IEEE*, vol. 1, pp. 579–584 vol.1, 1998.

[21] L. Bahl, J. Cocke, F. Jelinek, and J. Raviv, "Optimal decoding of linear codes for minimizing symbol error rate (corresp.)," *IEEE Transactions on Information Theory*, vol. 20, pp. 284 – 287, March 1974.

[22] D. Zhao, A. Dauch, and T. Matsumoto, "Bicm-id using extended mapping and repetition code with irregular node degree allocation," in *Vehicular Technology Conference, 2009. VTC Spring 2009. IEEE 69th*, pp. 1–5, 2009.

[23] P.-S. Lu, V. Tervo, K. Anwar, and T. Matsumoto, "Low-complexity strategies for multiple access relaying," in *IEEE 73rd Vehicular Technology Conference (VTC Spring)*, (Budapest, Hungary), pp. 1–6, May 2011.

[24] L. Hanzo, T. Liew, and B. Yeapi, *Turbo Coding, Turbo Equalisation and Space-Time Coding: For Transmission over Fading Channels*. John Wiley & Sons, West Sussex, 2002.

[25] L. L. Hanzo, R. G. Maunder, J. Wang, and L.-L. Yang, *Near-Capacity Variable-Length Coding: Regular and EXIT-Chart-Aided Irregular Designs*. John Wiley & Sons, West Sussex, 2010.

[26] M. Dohler and Y. Li, *Cooperative Communications: Hardware, Channel & Phy*. John Wiley & Sons, Ltd Press, 2010.

[27] I. S. Gradshteyn and I. M. Ryzhik, *Table of integrals, series, and products*. Elsevier/Academic Press, Amsterdam, seventh ed., 2007.

[28] Z. Wang and G. Giannakis, "A simple and general parameterization quantifying performance in fading channels," *Communications, IEEE Transactions on*, vol. 51, no. 8, pp. 1389–1398, 2003.

[29] L. Rubio, J. Reig, and N. Cardona, "Evaluation of nakagami fading behaviour based on measurements in urban scenarios," {*AEU*} - *International Journal of Electronics and Communications*, vol. 61, no. 2, pp. 135 – 138, 2007.

[30] S. ten Brink, "Convergence behavior of iteratively decoded parallel concatenated codes," *IEEE Transactions on Communications*, vol. 49, pp. 1727–1737, October 2001.

[31] S. Brink, "Code characteristic matching for iterative decoding of serially concatenated codes," *Annales Des Tlcommunications*, vol. 56, no. 7-8, pp. 394–408, 2001.

[32] K. Fukawa, S. Ormsub, A. Tlli, K. Anwar, and T. Matsumoto, "Exit-constrained bicm-id design using extended mapping," *EURASIP Journal on Wireless Communications and Networking*, vol. 2012, pp. 1–17, 2012.

[33] T. Cover, "A proof of the data compression theorem of slepian and wolf for ergodic sources (corresp.)," *Information Theory, IEEE Transactions on*, vol. 21, no. 2, pp. 226–228, 1975.

[34] A. E. Gamal and Y.-H. Kim, *Network Information Theory*. Cambridge University Press, 2011.